

AD-A102 088

OHIO STATE UNIV RESEARCH FOUNDATION COLUMBUS  
ELECTRON DEVICE CONTACT STUDIES.(U)  
AUG 80 P E WIGEN, M O THURSTON

F/G 20/12

F33615-77-C-1002

UNCLASSIFIED

AFWAL-TR-80-1130

NL

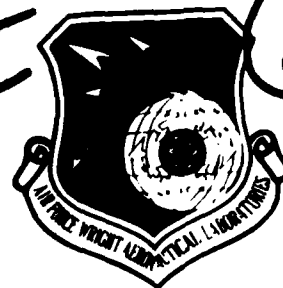
1-1-1  
AD  
A 102088

END  
DATE  
FILMED  
8-81  
DTIC

AD A102088

AFWAL-TR-80-1130

LEVEL II



2

ELECTRON DEVICE CONTACT STUDIES

Philip E. Wigen

Marlin O. Thurston

The Ohio State University Research Foundation  
1314 Kinnear Road  
Columbus, Ohio 43212

DTIC  
ELECTE  
JUL 28 1981  
S D

August 1980

TECHNICAL REPORT AFWAL-TR-80-1130

Interim Report for Period 1 November 1978 - 31 October 1979

Approved for public release; distribution unlimited.

DTIC FILE COPY

AVIONICS LABORATORY  
AIR FORCE WRIGHT AERONAUTICAL LABORATORIES  
AIR FORCE SYSTEMS COMMAND  
WRIGHT-PATTERSON AIR FORCE BASE, OHIO 45433

81 7 27 045

# NOTICE

When Government drawings, specifications, or other data are used for any purpose other than in connection with a definitely related Government procurement operation, the United States Government thereby incurs no responsibility nor any obligation whatsoever; and the fact that the government may have formulated, furnished, or in any way supplied the said drawings, specifications, or other data, is not to be regarded by implication or otherwise as in any manner licensing the holder or any other person or corporation, or conveying any rights or permission to manufacture use, or sell any patented invention that may in any way be related thereto.

This report has been reviewed by the Office of Public Affairs (ASD/PA) and is releasable to the National Technical Information Service (NTIS). At NTIS, it will be available to the general public, including foreign nations.

This technical report has been reviewed and is approved for publication.

*Millard G. Mier*

MILLARD G. MIER, Project Engineer  
Electronic Research Branch, AFWAL/AADR  
Avionics Laboratory

FOR THE COMMANDER

*Philip E. Stover*

PHILIP E. STOVER, Chief  
Electronic Research Branch, AFWAL/AADR  
Avionics Laboratory

"If your address has changed, if you wish to be removed from our mailing list, or if the addressee is no longer employed by your organization please notify AFWAL/AADR, W-PAFB, OH 45433 to help us maintain a current mailing list".

Copies of this report should not be returned unless return is required by security considerations, contractual obligations, or notice on a specific document.

| REPORT DOCUMENTATION PAGE  |                                      | READ INSTRUCTIONS<br>BEFORE COMPLETING FORM                                   |
|--|--------------------------------------|---|
| 1. REPORT NUMBER<br>AFWAL-TR-80-1130   | 2. GOVT ACCESSION NO.<br>AD-A102 088 | 3. RECIPIENT'S CATALOG NUMBER   |
| 4. TITLE (and Subtitle)<br><br>ELECTRON DEVICE CONTACT STUDIES.  |                                      | 5. TYPE OF REPORT & PERIOD COVERED<br>Interim Technical<br>11/1/78 - 10/31/79 |
|  |                                      | 6. PERFORMING ORG. REPORT NUMBER<br>764596-710525 ✓                           |
| 7. AUTHOR(s)<br>Philip E. Wigen and Marlin O. Thurston   |                                      | 8. CONTRACT OR GRANT NUMBER(s)<br>F33615-77 C-1002 ✓                          |
| 9. PERFORMING ORGANIZATION NAME AND ADDRESS<br>The Ohio State University<br>Research Foundation<br>1314 Kinnear Road, Columbus, Ohio 43212   |                                      | 10. PROGRAM ELEMENT, PROJECT, TASK<br>AREA & WORK UNIT NUMBERS                |
| 11. CONTROLLING OFFICE NAME AND ADDRESS<br>Avionics Laboratory, Air Force Wright Aeronauti-<br>cal Laboratories, Air Force Systems Command,<br>Wright-Patterson Air Force Base, Ohio 45433   |                                      | 12. REPORT DATE<br>Aug 1980   |
|  |                                      | 13. NUMBER OF PAGES<br>39   |
| 14. MONITORING AGENCY NAME & ADDRESS (if different from Controlling Office)  |                                      | 15. SECURITY CLASS. (of this report)<br><br>Unclassified                      |
|  |                                      | 15a. DECLASSIFICATION/DOWNGRADING<br>SCHEDULE                                 |
| 16. DISTRIBUTION STATEMENT (of this Report)<br>Approved for public release; distribution unlimited.  |                                      |   |
| 17. DISTRIBUTION STATEMENT (of the abstract entered in Block 20, if different from Report)   |                                      |   |
| 18. SUPPLEMENTARY NOTES  |                                      |   |
| 19. KEY WORDS (Continue on reverse side if necessary and identify by block number)<br><br>Contacts, Gallium Arsenide, Ohmic, Tunneling   |                                      |   |
| 20. ABSTRACT (Continue on reverse side if necessary and identify by block number)<br><br>This report describes the initial half of a program of investigation and characterization of contacts made to GaAs. A theoretical model of contact behavior based on electron tunneling is adapted to GaAs and will be used to compare experimental results of Au contacts fabricated on Sn diffused, n-type, GaAs surface layers. The fabrication of n-type layers using spin-on dopant sources and a semi closed chamber, in an open tube diffusion process are explained. The characterization of contact performance with a value of specific contact resistance, $R_c$ , and the measurement of $R_c$ using the transfer |                                      |   |

20. (Abstract) continued

length method are covered. Investigation into In-au GaAs alloyed type contacts is also presented.

# PREFACE

The research report contained herein was supported by the U.S. Air Force Avionics Laboratory, Wright-Patterson Air Force Base, Ohio, under contract No. F 33615-77-C-1002, "Electron Device Contact Studies." Research described in Section I and II was performed at The Ohio State University, Department of Electrical Engineering. Research covered in Section III was performed at The Ohio State University, Department of Physics. This report covers a period from November 1, 1978 to October 31, 1979.

The main objective of this research program is to investigate the fabrication of low resistance contacts to gallium arsenide (GaAs) and to examine their behavior with respect to theoretical models. This report covers the background theory used in the modeling of the contacts and gives the processing steps developed for the fabrication of Au-GaAs contacts.

|                           |  |
|---------------------------|--|
| <b>Accession For</b>      |  |
| NTIS GRA&I                | <input checked="checked" type="checkbox"/> |
| DTIC TAB                  | <input type="checkbox"/>                   |
| Unannounced               | <input type="checkbox"/>                   |
| Justification             |  |
| By                        |  |
| Distribution/             |  |
| <b>Availability Codes</b> |  |
| Dist                      | Avail and/or Special                       |
| A                         |  |

## TABLE OF CONTENTS

|   | Page   |
|---|--------|
| Section I    Research on tunneling behavior<br>in Au-GaAs contacts                        | 1      |
| 1.    Introduction  | 1      |
| 2.    Theoretical background of electron<br>tunneling and its relationship to<br>contacts | 2      |
| 3.    Experimental method and data  | 19     |
| 4.    Summary   | 28     |
| 5.    Appendix  | 29     |
| <br>Section II    Research on contact characteristics as<br>related to surface states     | <br>34 |
| 1.    Introduction  | 34     |
| 2.    Theoretical background  | 34     |
| 3.    Experimental method   | 35     |
| <br>Section III    Optical Measurements   | <br>37 |
| <br>References  | <br>38 |

## LIST OF ILLUSTRATIONS

| <u>Figure</u> |   | <u>Page</u> |
|---------------|---|-------------|
| 1             | Basic model for the metal-semiconductor contact   | 3           |
| 2             | Model for the metal semiconductor contact when the semiconductor is heavily doped               | 5           |
| 3             | Computer calculation of $R_c$ for various doping levels   | 11          |
| 4             | Contact structures used for determination of $R_c$ by the transfer length method                | 12          |
| 5             | Model used to determine $L_T$ and $R_c$ from the potential distribution of the conducting layer | 13          |
| 6             | Plot of $V(x)$ for the actual contact structure and determination of $L_T$                      | 15          |
| 7             | Photograph of the diffusion furnace set up  | 23          |
| 8             | Contact structure used to test for an n-type layer  | 24          |
| 9             | Current-voltage characteristics of the Al contacts A, B, and C of Figure 8                      | 24          |
| 10            | Photograph of the semi closed chamber used in the diffusion                                     | 27          |



## SECTION I

### 1. Introduction

Low resistance contacts, otherwise referred to as "ohmic" contacts, to GaAs are necessary if practical GaAs devices are to be realized. The term "ohmic" generally refers to a contact which exhibits non-rectifying current-voltage (I-V) behavior and an appropriately low value of resistance. The quantitative term used for describing the resistance of the contact is called "specific contact resistance,"  $R_c$ , and has units of  $\Omega\text{-cm}^2$ . The value of  $R_c$  gives a measure of the contact resistance in relation to its size. As the size of a contact is varied the absolute circuit resistance due to that contact changes but the value of  $R_c$  remains constant. Researchers currently working on the problem of making contacts to GaAs [1-6] report values of  $R_c$  in the range of  $10^{-3} - 10^{-7} \Omega\text{-cm}^2$  using various fabrication methods, and this is the range currently referred to as "ohmic."

Nearly all metals of practical interest, when applied to GaAs to form a contact, result in the formation of a Schottky barrier. According to simple theory, the barrier height is proportional to the difference between the work functions of the metal and the GaAs. Using this idea, the ohmic contact could be made by choosing an appropriate metal so that the work function difference would go to zero or even negative. However, due to the interaction of the metal and GaAs during contact formation [7,8], surface states are formed which always cause a barrier to be present and to have a height that is relatively independent of the choice of metal or the doping level within the GaAs.

In order to obtain an ohmic contact in the presence of a Schottky barrier, one must utilize the quantum mechanical phenomenon of tunneling. With this effect the electrons do not experience the barrier at the contact but tunnel through the barrier at points where the barrier width is sufficiently narrow. If the GaAs is highly doped then a sufficiently narrow barrier can be made so electrons tunnel through at room temperatures and low resistance contact behavior is observed.

Fabrication of ohmic contacts to GaAs has been explained as depending on tunneling to achieve ohmic properties but verification of the application of the tunneling model has not been completely shown to this point in time. This is due in part to the method by which currently used ohmic contacts are fabricated. In the case of a contact to n-type GaAs, an alloy of Au-Ge is put on the GaAs surface and heated. The Ge diffuses into the GaAs surface and creates a highly doped surface layer, giving rise to a narrow Schottky barrier width which allows tunneling. However, with such a process it is very difficult to determine exactly how the GaAs surface has been changed and to obtain the information about doping profile necessary to relate contact operation to the tunneling model.

Therefore, current information on GaAs contacts has been limited to either recipes on how someone made a contact with a certain value of  $R_c$  or theoretical calculations of contact performance based on the tunneling model without experimental verification. In the case of the former, even though an ohmic contact may be obtained, contact performance under various conditions, for example different temperatures, cannot be predicted but must be measured for each contact. Furthermore, a quantitative prediction of contact behavior under different conditions of fabrication (i.e., different metals or different semiconductor materials) cannot be made.

The aim of this part of the research program is to attempt to put both parts together. The fabrication process used is such that an ohmic contact based on the tunneling principle is expected, but the procedure used allows information needed for the application of the theoretical model to be obtained. Once adequately verified the model can then be used to predict further contact performance.

This report details the first half of the research program in which the necessary theory and the fabrication processes to be used were developed. Section II reviews the theoretical ideas concerning tunneling and its application to contacts. Section III covers the details of the experimental fabrication procedure and results obtained to date. Section IV summarizes the first year results and outlines the direction of research to be done during the second term. Section V discusses the computer program used to calculate a theoretical value of  $R_c$ . References are given at the end of the report.

## 2. Theoretical background of electron tunneling and its relationship to metal-semiconductor contacts.

The relationship between electron tunneling and contact resistance is best understood by first considering the model for a metal-semiconductor (MS) contact. A simple model for a MS contact in equilibrium is given in Figure 1. This figure shows the band diagram resulting from contact between a metal and a uniformly doped n-type semiconductor. The difference in work functions between the metal and semiconductor [9], as well as effects due to surface states, result in a potential barrier being formed of height  $\phi_B$  for electrons flowing from metal to semiconductor and of height  $\phi_{bi}$  for electrons from semiconductor to metal. This potential barrier is commonly called a Schottky barrier and also has associated with it at the surface of the semiconductor a space charge region of very low free electron concentration. The width of this effectively non-conducting region,  $W$ , is given by:

$$W = \sqrt{\frac{2\epsilon_s}{qN_D} \left( \frac{\phi_{bi}}{q} - \frac{kT}{q} \right)} \quad (1)$$

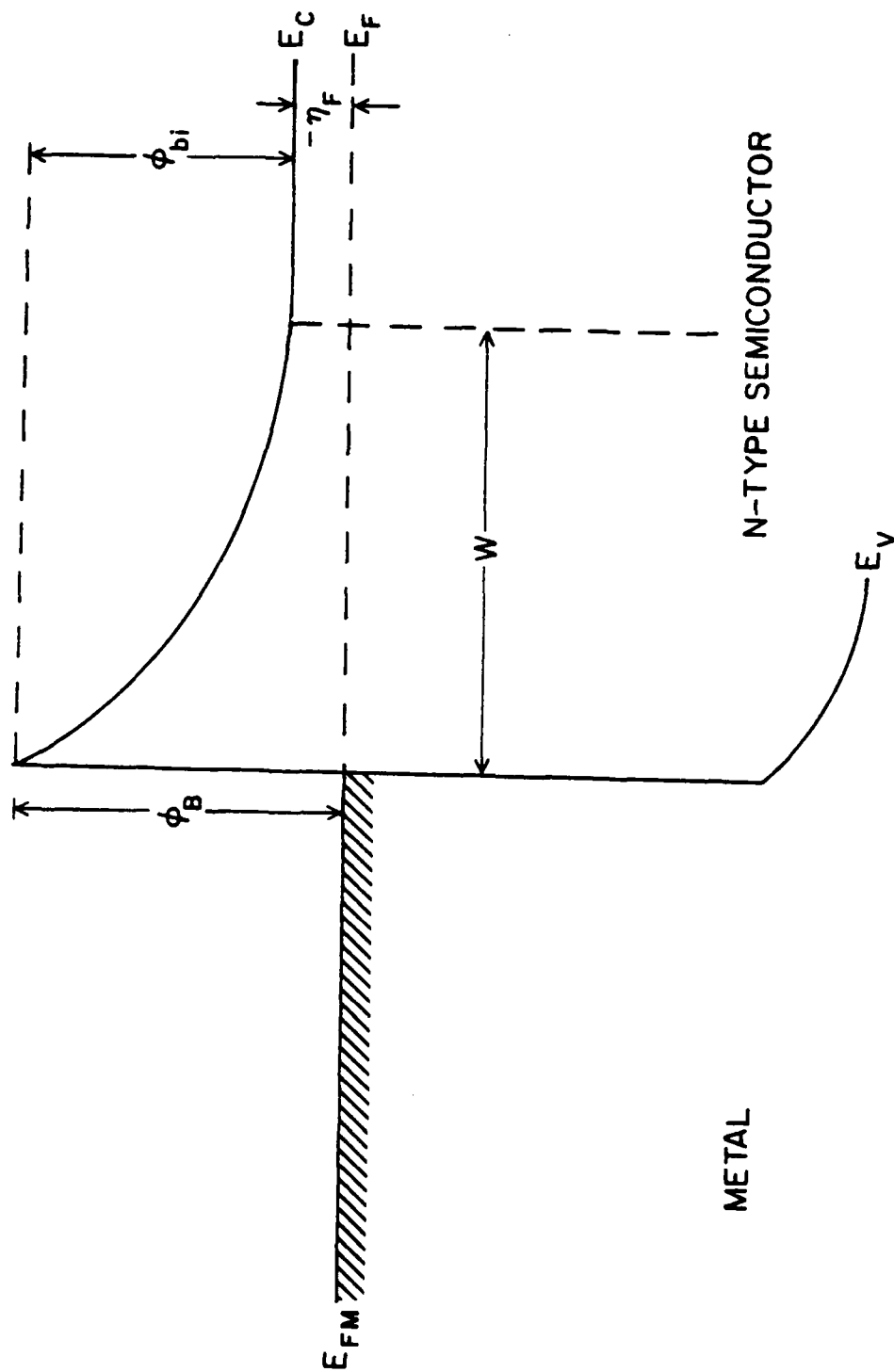


Figure 1. Basic model for the metal-semiconductor contact.

where  $\epsilon_s$  = semiconductor permittivity  
 $N_D$  = n-type donor doping concentration  
 $\phi_{bi}$  = "built in potential"  
 $k$  = Boltzmann's constant  
 $T$  = temperature  
 $q$  = electronic charge

The flow of electrons across the junction is determined by thermionic emission over the barrier. The barrier height,  $\phi_B$ , remains relatively constant and so the electron flow from metal to semiconductor is relatively constant and small except for extremely high temperatures. The flow in the opposite direction depends on  $\phi_{bi}$  which can be made smaller by an appropriate bias across the junction. In both cases, the barrier exhibits an impediment to electron flow and the contact exhibits high contact resistance. Specifically, the contact's characteristics are those of a metal semiconductor diode.

Classically,  $\phi_B$  is given by

$$\phi_B = \phi_M - X_s \quad (2)$$

where  $\phi_M$  = metal work function

$X_s$  = semiconductor electron affinity.

Therefore, a choice of metal giving  $\phi_m = X_s$  would lead to  $\phi_B = 0$  and no barrier, meaning a non rectifying, low resistance "ohmic" contact. However, due to surface states arising from reaction between the metal and semiconductor surface [9] a finite  $\phi_B$  will always exist, and therefore obtaining a low resistance contact in the presence of such a barrier is seemingly impossible.

To overcome this problem, the semiconductor is doped very highly giving a large  $N_D$  and the band diagram of Figure 2 will result. In this figure the semiconductor donor doping concentration,  $N_D$ , is so large that the fermi level in the semiconductor lies above the conduction band. In such a case, the semiconductor is said to be degenerate. This high doping affects the contact resistance through a reduction in  $W$  due to the increased  $N_D$ . For the case of  $T = 0^\circ K$ , with electrons concentrated in states around the fermi level in both metal and semiconductor, the thinness of  $W$  allows electrons to quantum mechanically tunnel through the potential barrier into available states on the other side. At even higher temperatures, the electrons move up the barrier by obtaining thermal energy and are presented with an even thinner barrier through which to tunnel. This process leads to a large flow of electrons across the junction without their having to go over the barrier. Such tunneling results in low contact resistance even when a Schottky barrier is present.

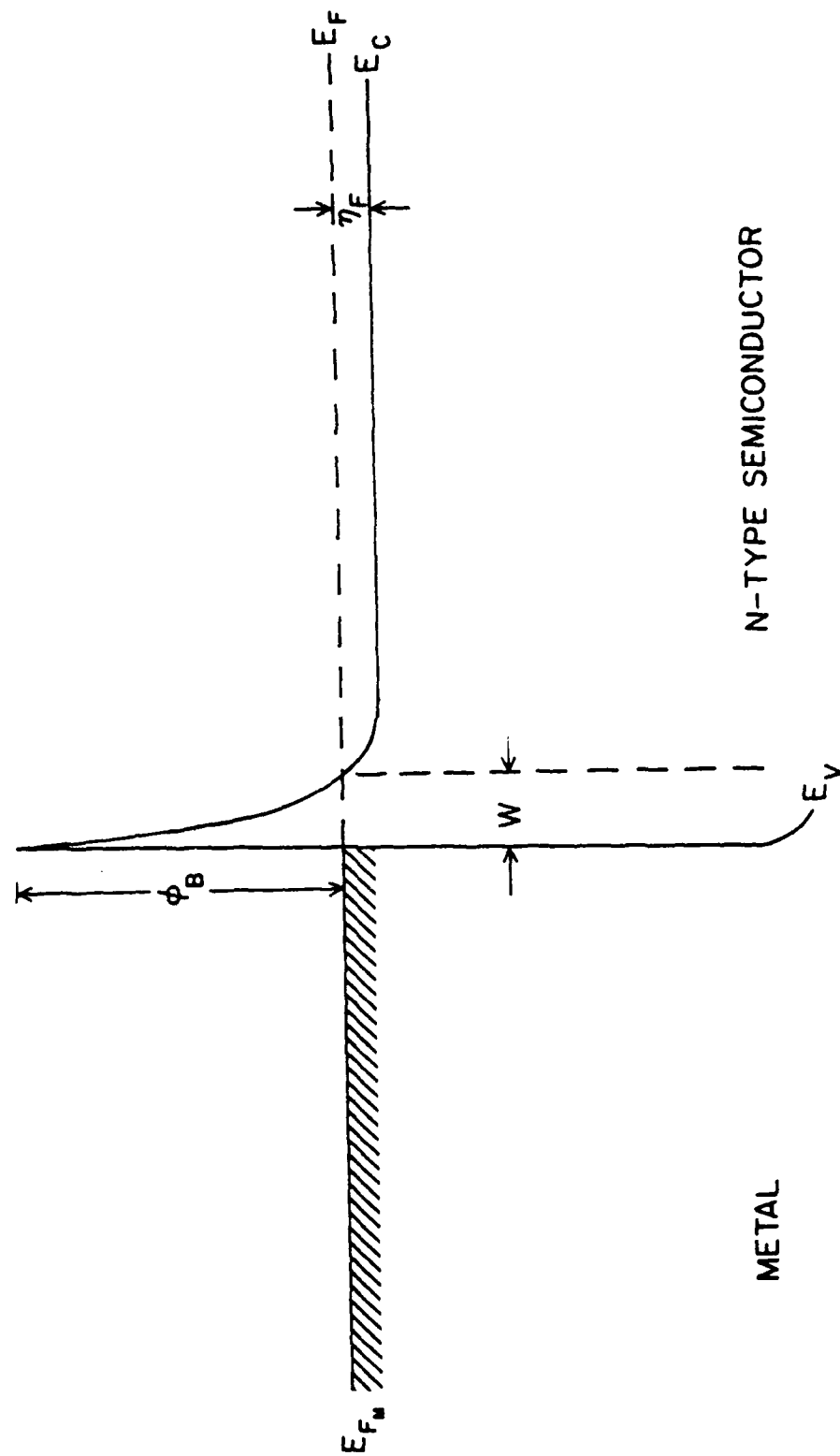


Figure 2. Model for the metal-semiconductor contact when the semiconductor is heavily doped. (degenerate)

Using a model similar to Figure 2, Padovani and Stratton [10] and Padovani [11] have developed theoretical equations giving the current-voltage response of an MS contact where electron tunneling through the insulating space charge region is the dominant conduction mechanism. The theoretical development begins with the equation [12, 13].

$$J = \left(\frac{2q}{h^3}\right) \int_0^\infty [f_1(E_1) - f_2(E_1)] \int P(E_1, p_y, p_z) dp_y dp_z dE_1 \quad (3)$$

giving a one dimensional current density for electrons starting in conductor 1 (fermi function  $f_1(E)$ , electron energy  $E_1$ ) and tunneling through the barrier in to conductor 2. The term  $P(E_1, p_y, p_z)$  is the transmission probability for the electron. Applying the WKB approximation to the Schottky barrier to find  $P(E_1, p_y, p_z)$  gives

$$\ln P = -\frac{2}{h} \int_{x_1}^{x_2} [(P_x)^2] dx \quad (4)$$

when  $x_1$  and  $x_2$  are the reference points for the barrier where  $p_x^2 = 0$ .

Even if the WKB approximation is used, further simplifications are necessary to keep the mathematics tractable. One method is to limit discussion to certain conditions from which certain simplifying assumptions can be made, namely to consider tunneling from fermi level to fermi level and make Taylor expansions of the tunneling probability around the fermi level [14].

Such a limitation gives a more easily solvable expression for  $\ln P$  in terms of the coefficients in the Taylor expansion. The calculation of these coefficients involves integrating the various derivatives of electron momentum  $p(E)$  between the edges of the barrier,  $x_1$  and  $x_2$ . Therefore, a further assumption as to the nature of the momentum - energy relationship must be made using the following assumptions:

1. parabolic momentum - energy relationship with  $p=0$  referred to electrons at the semiconductor fermi level,  

$$(\bar{p}^2)|_{E=E_F} = 2m^*(E_1 - E_F)$$
2. semiconductor with uniform donor doping density,  $N_D$ , leading to a parabolic potential barrier in the semiconductor
3. neglect the image force correction to the barrier
4.  $\eta_F \ll \phi_B$       $\eta_F$  = fermi potential in the semiconductor

The values for the Taylor expansion coefficients become:

$$b_1 = \phi_B - qV/E_{oo} \quad (5)$$

$$c_1 = \frac{1}{2E_{oo}} \ln \frac{4(\phi_B - qV)}{\eta_F} \quad (6)$$

$$f_1 = \frac{1}{4E_{oo}\eta_F} \quad (7)$$

The subscript, 1, refers to electrons starting in the semiconductor. The term  $E_{oo}$  is the characteristic energy relating to tunneling:

$$E_{oo} = \frac{q\hbar}{2} \sqrt{\frac{N_D}{m^*e_s}} \quad (8)$$

From another viewpoint  $E_{oo}$  is seen to be inversely proportional to the space charge region width. Therefore, a higher  $E_{oo}$ , corresponding to a thinner  $W$ , means a larger likelihood that tunneling will occur.

For small applied biases,  $V$ , (we will be concerned with contact resistances in the limit as  $V \rightarrow 0$ ), with  $\exp[\eta_F - qV]/kT \ll 1$ , the expression for the current due to electrons flowing from the semiconductor to the metal (forward bias) is

$$J = \left[ \frac{A}{(c_1 kT)^2} \right] \exp[-b_1] \{ [\pi c_1 kT / \sin \pi c_1 kT] \\ \times [1 - \exp(-c_1 V)] - c_1 V \exp(-c_1 \eta_F) \} \quad (9)$$

This expression is also approximately valid for electrons flowing under reverse bias in the limit of reverse bias  $V \rightarrow 0$  and therefore the above equation can be used for both cases.

Equation (9) is valid for condition of  $\phi_B$ ,  $N_D$ , and  $T$  such that

$$\frac{1}{kT} - c_1 > \sqrt{2f_1} \quad (10)$$

Using equations (9) and (10) along with the definition for specific contact resistance,

$$R_c = \frac{dV}{dJ} \Big|_{V=0} \quad (11)$$

Yu [15] has determined that for the condition when equation (10) is satisfied

$$R_c = \left[ \frac{A \pi q}{kT \sin(\pi c_1 kT)} \exp\left(\frac{-\phi_B}{E_{oo}}\right) - \frac{A c_1 q}{(c_1 kT)^2} \exp\left(\frac{-\phi_B}{E_{oo}} - c_1 \eta_F\right) \right]^{-1} \quad (12)$$

where  $A = \frac{q 4 \pi m^* (kT)^2}{h^3}$  is the Richardson coefficient.

The region where equation (10) is satisfied, with electrons tunneling at the fermi level, is known as field emission (FE). Field emission is seen at room temperature only for very denegate doping and at very low temperatures for moderately doped samples.

For conditions of  $T$ ,  $\phi_B$ , and  $N_D$  for which eq.(10) is not satisfied a different regime of tunneling is encountered. This case is known as thermionic field emission (TFE) or thermally assisted tunneling. With TFE, conditions are not such that electrons can tunnel through at the fermi level, but electrons obtain thermal energy and move up the barrier to where they see a thinner barrier through which they can tunnel.

For the TFE case the I-V relationship is determined as in the FE case except that the Taylor expansion coefficients are not determined around the fermi level but at an energy  $E_m$  which is the position of the peak of the energy distribution of the emitted electrons.

The I-V response for the TFE case has been determined by Padovani and Stratton [10] and also by Padovani [11] and neglecting the effect of an erf term is given by

$$J = J_s \exp (qV/E_o)$$

$$\text{where } E_o = E_{oo} \coth E_{oo}/kT \quad (13)$$

$$\text{and } J_s = \frac{A \sqrt{\pi (\phi_B - qV + \eta_F) E_{oo}}}{kT \cosh(E_{oo}/kT)} \exp \left[ \frac{\eta_F}{kT} - \frac{\phi_B + \eta_F}{E_o} \right]$$

These equations are applicable around zero bias if

$$kT > 2E_{oo} [\ln(4\phi_B/\eta_F)]^{-1} \quad (14)$$

$$\text{and } \frac{\cosh^2(E_{oo}/kT)}{\sinh^3(E_{oo}/kT)} < \frac{2(\phi_B + \eta_F)}{E_{oo}} \quad (15)$$



Again using the definition for  $R_c$  around zero bias

$$R_c = \left. \frac{dV}{dJ} \right|_{V=0}$$

and taking the dominant term as the  $\exp V/E_0$  term then

$$R_c = \frac{E_0}{q} \left[ \frac{kT \cosh E_{00}/kT}{A \sqrt{\pi(\phi_B + \eta_F)E_{00}}} \right] \exp \left[ \frac{\phi_B + \eta_F}{E_0} - \frac{\eta_F}{kT} \right]$$

This equation is the same as the equation for  $R_c$  during TFE derived by Yu [15] except he used a J-V expression derived by Crowell and Rideout [16] which resulted in an effective substitution of  $E_0 = kT \sqrt{\coth E_{00}/kT}$  in the numerator in place of the previously defined  $E_0$  from equation (13). For a range in  $N_D$  of  $10^{18}/\text{cm}^3$  to  $10^{19}/\text{cm}^3$  the difference is only about a factor of two.

In the range where neither equation (10) nor (14) are satisfied, it would seem that neither FE nor TFE occur. However, this is not necessarily true. The fact is that over this narrow range the method of using a Taylor expansion to solve for the I-V equation merely does not give accurate results because coefficients are not accurate. Nevertheless, the actual  $R_c$  will lie between the values predicted by equations (12) and (16) and a smooth curve can be fitted.

The range for which equation (15) is not satisfied is called the thermionic emission (TE) regime. In this range tunneling does not occur and electron flow is dominated by emission over the barrier. This region is characterized by very large contact resistance with

$$R_c = \frac{kT}{qA} \exp \frac{\phi_B}{kT} \quad (17)$$

For this research program, the main thrust is to investigate whether or not the tunneling model can be used in determining  $R_c$  for the Au-GaAs contact. Figure 3 shows the results of an example computer calculation for  $R_c$  using the previous equations. Parameters for the calculation are  $\phi_B$ ,  $T$ , and  $N_D$ . Once actual contacts are shown to operate according to the model, the theory can be used to predict contact performance over a range of temperatures. Or from a fabrication viewpoint, the donor doping needed to give desired performance over a specific temperature range can be determined. The Appendix contains further information on the computer calculation.

#### Determination of $R_c$

There are various methods which can be used to measure  $R_c$  [17, 18]. The method used for this program is attributed to Schockley and known as the transfer

length method [19]. Yu [15] used this method to investigate contacts made to Si, and Hower, et al. [19] used it for As/In/Ge contacts to GaAs. The basic contact structure is shown in Figure 4.

The large square areas at either end are the contacts to be tested. The MS junction is formed between each end pad and the conducting substrate beneath. The overall structure forms a resistor with points between the ends where voltage can be picked off (small narrow contacts) to determine the sheet resistivity of the conducting layer.

A mathematical treatment of how such a structure can be used to determine contact resistance has been given by Hower, et. al. [19]. The analysis is based on a model of the contact as shown in Figure 5.

The term  $R_{\square}$  is the sheet resistivity of the n-type conducting layer. The term  $R_c$  is the specific contact resistance associated with the MS contact. For the test, a current  $I$  flows through the conducting n-type layer and out the contact which is connected to  $V=0$ . At the leading edge of the contact,  $x=0$ , the current entering the layer under the contact is given by

$$I(0) = - \frac{Z}{R_{\square}} \frac{dV(x)}{dx} \quad (18)$$

where  $Z$  is the width of the contact structure. At points to the right of this edge some current is drawn off due to  $R_c$ . At the point  $x=x_1$  the current remaining in the conducting layer is

$$I_1 = I(x=x_1) = - \frac{Z}{R_{\square}} \frac{dV}{dx} \Big|_{x=x_1} \quad x_1 \geq 0 \quad (19)$$

which is less than  $I(0)$  due to the amount lost into the contact. The current lost through  $R_c$  at  $x = x_1$  in an interval  $dx$  is

$$dI_1 = - \frac{Z}{R_{\square}} dxV(x_1) \quad (20)$$

Using (19)

$$\frac{dI}{dx} = - \frac{Z}{R_{\square}} \frac{d^2V(x)}{dx^2} \Big|_{x=x_1}$$

or

$$dI = - \frac{Z}{R_{\square}} \frac{d^2V(x)}{dx^2} dx \Big|_{x=x_1}$$

which must be equal to  $dI_1$ . Therefore

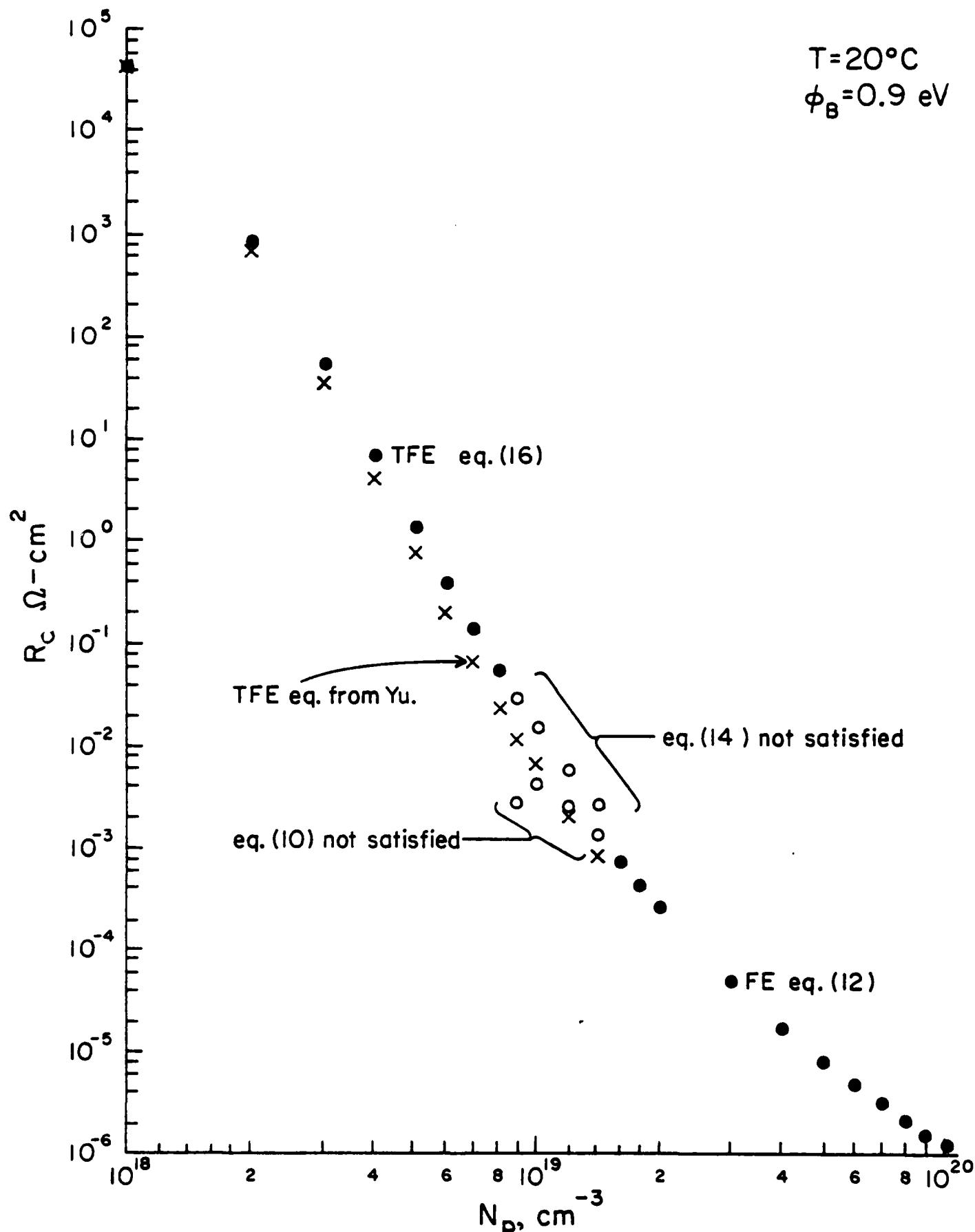
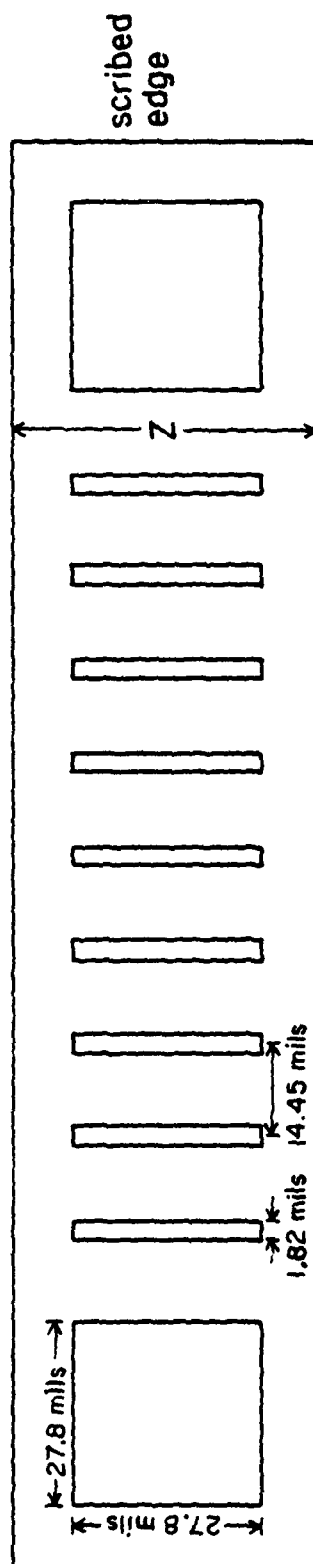


Figure 3. Computer calculation of  $R_c$  for various doping levels.



TOP VIEW

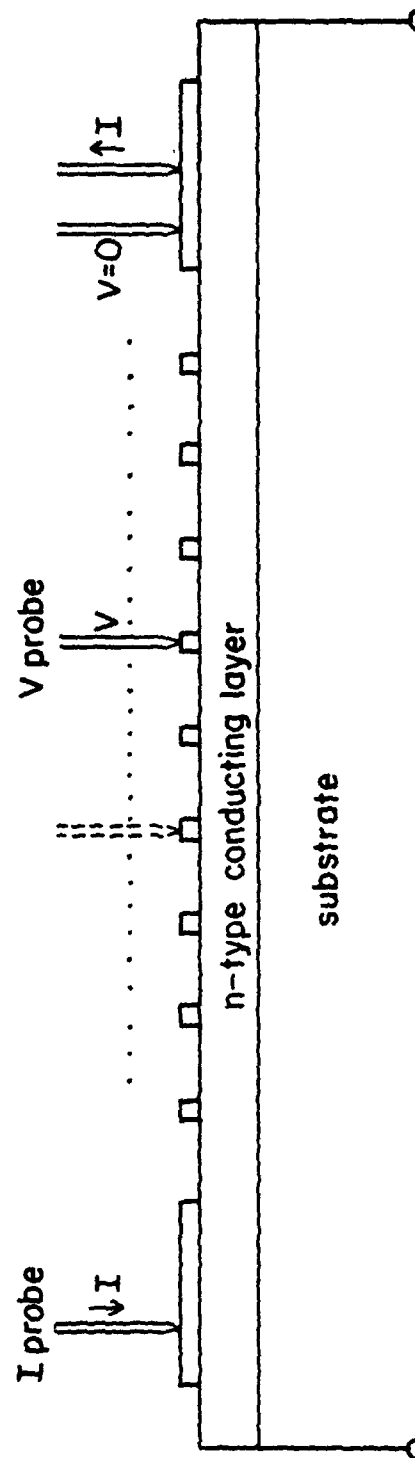


Figure 4. Contact structure used for determination of  $R_c$  by the transfer length method.

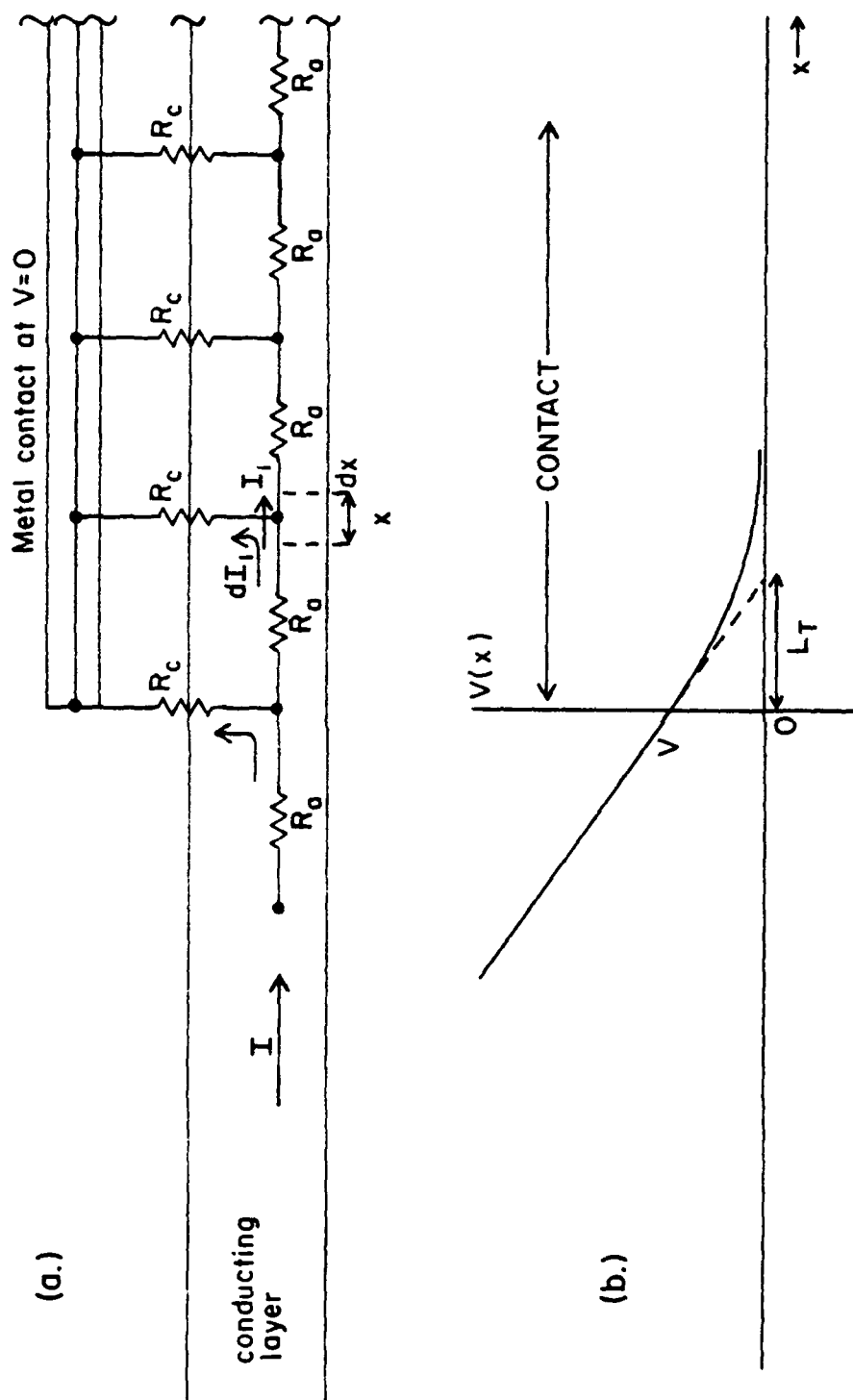


Figure 5. Model used to determine  $L_T$  and  $R_c$  from the potential distribution in the conducting layer.

$$\frac{-Z}{R_C} \frac{d^2V(x)}{dx^2} dx = - \frac{Z}{R_C} dxV(x)$$

or

$$\frac{1}{R_C} \frac{d^2V(x)}{dx^2} - \frac{1}{R_C} V(x) = 0 \quad x \geq 0 \quad (21)$$

which has the solution

$$V(x) = V_0 \exp (-x/L_T) \quad x \geq 0 \quad (22)$$

where

$$L_T = \sqrt{R_C/R_{\square}} \quad (23)$$

and is called the transfer length.  $V(x)$  is plotted in Figure 5 (b) for  $x \geq 0$ .

If a plot of  $V(x)$  is made for  $x < 0$  and the slope continued past  $x = 0$ , the intersection of the continued line with the  $x$  axis gives  $L_T$ . The values for  $V(x)$  for  $x < 0$  are determined by measuring the voltages at the thin pick off contacts along the contact structure. If the width of the pick off contacts is small compared to their separation, the voltage at one of these contacts can be considered to be the voltage along a line at the center of the pick off strip. An example of typical test is shown in Figure 6. The value of  $R$  is determined from the slope of the line, the dimension of the contact structure, and the current magnitude.

$$R_{\square} = - \frac{Z}{I} \frac{dV(x)}{dx} \quad x < 0 \quad (24)$$

Using this particular structure, the electron flow is from metal to semiconductor for the grounded end contact and from semiconductor to metal for the other contact into which current enters. Strictly speaking, the different directions of flow give different I-V characteristics and should give different values of  $R_C$ , but, as mentioned before, in the limit where the contact bias approaches zero, the I-V equations become nearly equal and so nearly equal values of  $L_T$  are seen for both contacts. A large difference in  $L_T$  under near zero bias conditions indicates contact non-uniformity probably related to problems with processing.

To compare the experimental data with theory the parameters of  $T$ ,  $\phi_B$  and  $N_D$  are needed. A direct measurement of  $\phi_B$  is possible but usually a set of curves for various  $\phi_B$  are developed and the experimental data for  $R_C$  is plotted in among the set of curves to compare the fit. The temperature,  $T$ , is usually not considered a control parameter in the sense that you adjust  $T$  to give a desired  $R_C$ . Usually  $\phi_B$  and  $N_D$  are controlled to give a desired  $R_C$  under certain conditions of  $T$ . In this sense the main parameter other than  $\phi_B$  is the doping of the substrate  $N_D$ .

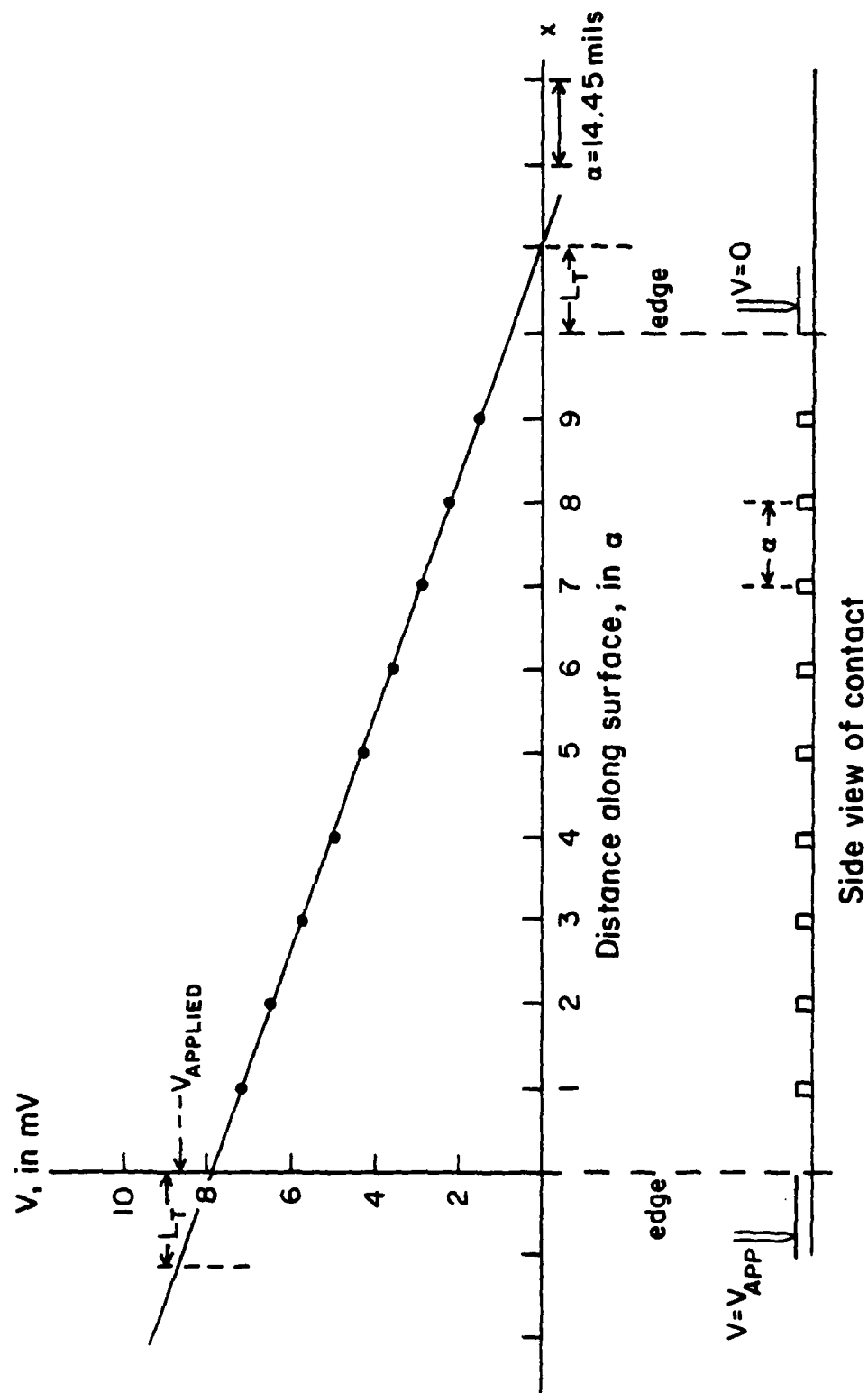


Figure 6. Plot of  $V(x)$  for the actual contact structure and determination of  $L_T$ .

Most experiments measuring  $R_c$  for MS contacts are concerned with n-type layers of fixed, uniform concentration  $N_D$  and this is why the theoretical model has been developed. However, it is rather hard to collect many data points to develop experimental curves relating  $R_c$  and  $N_D$  using uniformly doped layers due to the difficulties in fabricating such layers. Besides, actual tunneling contacts for practical applications are made using a diffused layer instead of a uniform layer. In such a diffused layer, the surface concentration of dopants immediately beneath the metal,  $C_s$ , is large thus giving rise to tunneling.

For this research program, instead of using a uniform surface layer, an n-type diffused layer is used to make the MS contacts. For insulation of the n-type layer from the rest of the substrate, a reverse biased pn junction is used. Namely, an n-type layer is diffused into the surface of a p-type semiconductor. During testing, the p-type layer remains at ground potential and the reverse biased pn junction between the n-type surface layer and p-type substrates confines current flow to the n-type layer as desired.

Using a diffused layer presents no problem with respect to measuring  $R_c$  using the transfer length method. For the diffused layer, an  $R_\square$  can be determined. However, in this case the  $R_\square$  represents an equivalent average for the entire layer and is still found from the slope of the  $V$  vs.  $x$  plot.

There is somewhat more of a problem in defining the donor dopant concentration to be used for  $N_D$ . The actual dopant profile in the n-type layer can be given as [20].

$$C(x) = C_s \operatorname{erfc} \frac{x}{2\sqrt{Dt}} \quad (25)$$

where  $D$  = diffusion coefficient of the dopant atom in GaAs  
 $t$  = time of diffusion  
 $C_s$  = dopant surface concentration  
 $x$  = depth into the surface

Because the dopant profile is not a uniform  $N_D$  the shape of the potential barrier at the MS junction is not parabolic and therefore the previously derived theory for  $R_c$  is not strictly applicable. A rigorous treatment would involve integrating the erfc profile twice, using Poisson's relation to find the potential barrier shape, and then finding a suitable approximation to use to predict the tunneling probability. The mathematics of this process is quite complicated so for this program a simple substitution of  $C_s$  for  $N_D$  is used as a first order approximation.

A feeling for exactly how much of an approximation this creates can be gotten by examining the change in dopant concentration due to the erfc profile over the region in interest, namely the space charge region. Some typical parameters for a diffusion of Sn into GaAs to form the n-type layer are



$$C_s \approx 10^{18}/\text{cm}^3 \quad [29]$$

for Sn in GaAs

$$D \approx 5 \times 10^{-14} \text{cm}^2/\text{sec} \quad [21]$$

$$t = 3 \text{ hrs.}$$

$$\phi_B \approx 0.9 \text{ eV}$$

For  $\phi_B \gg \eta_F$  and  $\phi_B \approx \phi_{bi}$  (the built in potential of the barrier).

A calculation for the width of the space charge region, the important parameter in tunneling, assuming a uniform doping of  $C_s$  gives

$$W = \sqrt{\frac{2\epsilon_s}{qC_s} \left( \frac{\phi_B}{q} - \frac{kT}{q} \right)}$$

$$W \approx \sqrt{\frac{2(12)(8.85)(10^{-14})}{(1.6)(10^{-10})(10^{18})} (0.9 - 0)}$$

$$W \approx 3.5 \times 10^{-6} \text{ cm.}$$

The actual Sn atom doping profile is given by

$$C(x) = C_s \operatorname{erfc} \frac{x}{2\sqrt{Dt}}$$

$$= 10^{18} \operatorname{erfc} \frac{x}{4.6 \times 10^{-5}} \quad \text{for } x \text{ in cm.}$$

Therefore, for  $x = W = 3.5 \times 10^{-6} \text{ cm}$

$$C(w) = 10^{18} \operatorname{erfc}(7.6 \times 10^{-2})$$

or

$$C(w) \approx 9.2 \times 10^{17}/\text{cm}^3.$$

Therefore, based on the width of the space charge region in a uniformly doped sample with  $N_D = C_s$ , the actual doping concentration in the diffused sample has a variation of approximately 8%. This means that the actual  $W$  is slightly larger and therefore the tunneling probability is slightly less. However, with only an 8% variation in concentration over the space charge width, the change in  $W$  from that obtained with an exact calculation is slight and the change in tunneling probability would also be slight. Moreover, for TFE where electrons tunnel at energies above  $E_F$  and go into the conduction band while still within the space charge region, the concentration change over their tunneling distance is even less.

This means that the barrier shape they see is even closer to that of the uniformly doped case and the theory should be even closer. Therefore, in view of the extreme simplification of the mathematics at a cost of an error on the order of 8%, the substitution of  $C_S$  from the diffused profile for  $N_D$  seems justified.

Because of its ease of fabrication, there is another benefit in using a diffused layer. The value of  $C_S$  is easily varied by incorporating changes into the processing step at the point the dopant is applied to the semiconductor. More details are given in the section covering experimental procedure.

With the particular processing method used for this research, the value of  $C_S$  is not known beforehand but must be determined experimentally. The method used utilizes the knowledge that the doping profile goes as eq. (25). As mentioned before, the n-type layer is diffused into a p-type substrate. The background concentration of the substrate,  $C_B$ , is known. Assuming complete ionization of the n-type donors, a p-n junction is formed where the n-type concentration of the layer is equal to the background p-type concentration. Using equation (25)

$$C(x = x_j) = C_B = C_S \operatorname{erfc} \frac{x_j}{2\sqrt{Dt}}$$

where  $x_j$  = junction depth = thickness of the n-type layer. Since  $C_B$ ,  $D$ , and  $t$  are known, if  $x_j$  can be measured,  $C_S$  can be determined.

An angle lapping and staining procedure is used to measure  $x_j$ . After the diffusion is performed, a piece of the diffused wafer is scribed out and placed on a lapping jig. Using alumina powder on a glass plate, the edge of the piece is lapped down at a shallow angle  $\approx 3^\circ$  such that the semiconductor substrate beneath the original diffused surface is exposed. A staining solution is applied to this lapped surface and under illumination a reaction occurs whereby the p-type layer differs in color from the n-type layer. This step is referred to as junction delineation. After the staining is complete, the lapped and stained junction area is viewed under a microscope with an attached interferometer. By noting the deflection of the interference fringes across the lapped area with respect to the original diffused surface, the depth of the junction,  $x_j$ , can be determined. Equation (25) is then used to calculate  $C_S$ .

The value of  $C_S$  can also be determined by a measurement of the average resistivity,  $\bar{\rho}$ , of the diffused layer and relating it to a curve, commonly known as an Irvin curve [22], which gives  $C_S$  for a measured value of  $\bar{\rho}$  when the shape of the diffused profile is known. The value of  $\bar{\rho}$  is calculated from

$$\bar{\rho} = R_{\square} x_j \quad (26)$$

where  $R_{\square}$  is obtained during the measurement of  $R_c$ .

In other terms,

$$\bar{\rho} = \frac{1}{\sigma} \quad (27)$$

where  $\sigma$  is the average conductivity. For a uniformly doped n-type layer, neglecting the contribution of holes.

$$\sigma = q\mu_n ND \quad (28)$$

where  $\mu_n$  = electron mobility.

For a diffused layer where the number of electrons varies with depth into the semiconductor according to equation (25), an integration must be used. Namely,

$$\sigma = \frac{q}{x_j} \int_0^{x_j} \mu_n(x) N(x) dx \quad (29)$$

For the diffused layer

$$N(x) = C(x) = C_s \operatorname{erfc} \frac{x}{2\sqrt{Dt}}$$

and the mobility becomes a function of  $x$  since mobility depends on concentration. Baliga [23] has used a computer to perform the integration and determined sets of curves relating  $\bar{\sigma}$  to  $C_s$  for different values of  $C_B$  (which determine  $x_j$ ). Using these curves, a measurement of  $R_{\square}$  and  $x_j$  can yield a cross check on the value of  $C_s$ .

However, there may be some problems with relating such curves directly to GaAs. In his calculation, Baliga assumed complete ionization of the n-type dopant. Complete ionization assumes that the number of conduction electrons,  $n$ , is much less than the effective density of states,  $N_c$ , in the conduction band. Since  $N_c$  is proportional to the electron effective mass,  $m_e^*$ , and in GaAs since  $m_e$  is very small  $N_c$  is also small. This means that at the doping levels needed to give low  $R_{\square}$ , an assumption of complete ionization may give  $n \approx N_c$  which would invalidate such an assumption. A modification of the  $\bar{\sigma}$  vs.  $C_s$  curve, taking into account incomplete ionization, may be possible and some investigation will be performed along this direction.

Other methods such as Auger analysis are also currently being looked into as a possible way of determining  $C_s$ .

### 3. Experimental Method and Data

The general method for fabrication of the contact structures will be explained in this section. Processing begins with a p-type GaAs wafer into which an n-type layer is diffused. Using a photoresist lift off technique, a delineated Au contact structure is then fabricated. Finally the individual contact structures are scribed out and tested.

The GaAs wafer substrates were obtained from Crystal Specialities, 419 West Maple Ave., Monrovia, Ca. 91016. The manufacturers specifications were:

P-type - Zn doped

Carrier Concentration -  $5 \times 10^{16}/\text{cm}^3$

Mobility -  $378.6 \text{ cm}^2/\text{V-sec}$

Orientation - (100)

Resistivity -  $0.37 \Omega\text{-cm}$

Wafer thickness - 17 mils

One side polished

A total of six wafers were obtained. Small sections from each wafer were scribed out and cleaned in Trichloroethylene, Acetone, Methanol, and  $\text{H}_2\text{O}$  and each was tested for carrier concentration and mobility using a van der Pauw technique [24]. Ohmic contacts were made to the perimeter of the sample by applying small dots of In-2% Zn alloy [25] and heating in a furnace at  $T = 225^\circ\text{C}$  for 10 min. After the 10 min, the melted dots were slightly rubbed into the surface of the wafer to give better adhesion. The following data were obtained from the van der Pauw measurements.

| Wafer # | Average resistivity<br>$\Omega\text{-cm}$ | Hall mobility<br>$\text{cm}^2/\text{V-sec}$ | Background Zn concentration<br>$/\text{cm}^3$ |
|---------|---|---|---|
| 3A-1    | 0.165                                     | 193.7                                       | $1.95 \times 10^{17}$                         |
| 4A-1    | 0.24                                      | 236.7                                       | $1.1 \times 10^{17}$                          |
| 5A-1    | 0.146                                     | 213.5                                       | $2 \times 10^{17}$                            |
| 6A-1    | 0.144                                     | 222   | $1.96 \times 10^{17}$                         |
| 7A-1    | 0.146                                     | 215.5                                       | $1.98 \times 10^{17}$                         |
| 8A-1    | 0.252                                     | 241.7                                       | $1.03 \times 10^{17}$                         |

The background concentration  $C_B$  was calculated using

$$C_B = \frac{1}{q\mu_H\bar{r}} \quad (30)$$

This assumes that the Hall and drift mobilities for holes are the same and is the usual assumption [26].

Before the diffusion, the wafers are given the following wash and etch treatment.

- |   | <u>Time</u>                        |
|---|------------------------------------|
| 1. Wash in trichloroethylene (TCE)  | 30 sec + 30 sec ultrasonic cleaner |
| 2. Wash in acetone (ACE)  | same as above                      |
| 3. Wash in methanol (MET)   | same as above                      |
| 4. Rinse and soak in deionized, distilled H <sub>2</sub> O while preparing next step etch                   |                                    |
| 5. MB etch<br>1 HF : 1 HCl : 4H <sub>2</sub> O + 1 drop<br>H <sub>2</sub> O <sub>2</sub> /10 ml of solution | 2 min                              |
| 6. Wash in high purity 18 MΩ H <sub>2</sub> O   |                                    |
| 7. Blow dry with purified N <sub>2</sub>  |                                    |
| 8. Dry under heat lamp  |                                    |
| 9. Store in petri dish  |                                    |

The MB etch step is reported to result in the least number of surface defects [1].

The above steps were performed on every wafer that was diffused. However, the subsequent steps of making and actual diffusion were varied throughout the course of this first year until suitable results were obtained. Much of the research effort this first year went into solving problems with the diffusion process. The following discussion explains the various techniques investigated during this period.

The basic diffusion process consists of using Sn as the dopant to form the n-type layer on the surfact. The furnace is an open quartz tube type shown in Figure 7. During the diffusion, Ar gas is taken through a cold trap (dry ice in a dewar) to condense out any trace of moisture and then put into the diffusion chamber. The opposite end of the diffusion tube goes into a scavenger box which collects and exhausts the gas. During diffusion, As is given off from the GaAs wafer and needs to be exhausted since it is poisonous.

The source for the Sn is a spin on dopant, Tinsilicafilm, manufactured by Emulsitone Company, 19 Leslie Court, Whippany, N.J. 07981. When this solution is spun onto the GaAs wafer and densified by heating, a SiO<sub>2</sub> film incorporating Sn is formed on the surface. During diffusion the Sn in the film goes into the GaAs surface and forms the n-type layer. Manufacturer's data states that surface concentrations of 10<sup>20</sup>/cm<sup>3</sup> are possible, which is enough to give appreciable tunneling.

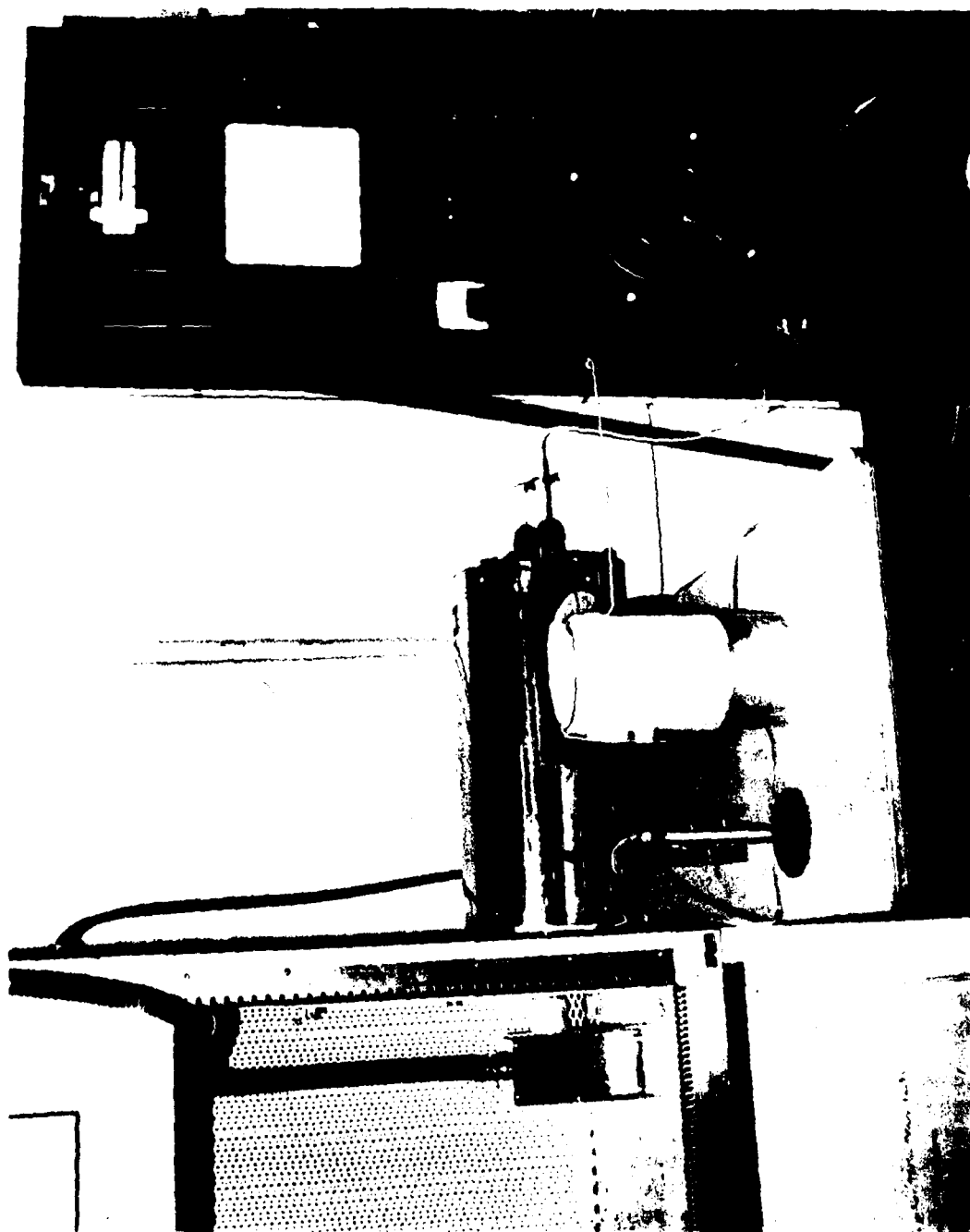


Figure 7. Photograph of the diffusion furnace.

The dense  $\text{SiO}_2$  film formed on the surface supposedly acts as a barrier to the outdiffusion of As from the GaAs wafer and should allow a totally open tube diffusion to be performed.

For the first diffusion trial, an appropriate set of masks was made to allow the fabrication of three rectangular n-type islands in the p-type GaAs substrate. With such islands, there would be p-n junction isolation on all sides of the n-type diffusion on which the metal contact structures would be formed.

The first processing step for this trial was the application and densification of Emulsitone's Glass Forming Solution #306. This solution forms a dense glass which would prevent the diffusion of Sn into the GaAs in the areas to be left p-type. The first mask was then used in a photolithographic step to etch rectangular holes in this glass layer.

One of the two wafers of this first trial was further processed with an application of diluted, Emulsitone Silicafilm. The Silicafilm forms a layer of  $\text{SiO}_2$  with no dopants and is normally used for surface passivation. According to the manufacturer, an application of Silicafilm solution, diluted with ethyl alcohol, will give a thin layer of  $\text{SiO}_2$  which will prevent surface pitting due to loss of As, while still allowing the dopants in the dopant film to diffuse through.

Finally, the layer of Tinsilica dopant was applied to both of the wafers and the wafers were put into an open boat and inserted into the diffusion furnace. The diffusion temperature was  $850^\circ\text{C}$  and the time was 2 hrs. Visual inspection of these wafers after the diffusion yielded the following:

1. The area of the GaAs surface under the Glass Forming Solution was severely damaged through some sort of chemical reaction during diffusion.
2. The wafer without the intermediate diluted Silicafilm layer showed pitting. The other wafer showed traces of surface pitting.

Because of 1, it was decided that the Glass Forming Solution would not be used further. This would not allow the fabrication of islands so another structure was necessary. Other investigators [19], have used mesa etched structures when investigating similar contact structures. However, due to the ease with which GaAs can be scribed and the smoothness of the resulting edge cleave, it was felt that contact structures fabricated with p-n junction isolation only on the bottom and then scribed apart into rectangles would be sufficient. Such a method allows for a very even diffusion of Sn into the entire surface of the GaAs substrate. Metal contact structures would then be made on the diffused surface and the individual structures scribed apart for testing. This method also allows for more structures to be made at one time on the same amount of surface.

Using this second method of entire surface diffusion, several diffusion trials were performed. The intermediate layer of dilute Silicafilm was used in all trials and in the same open boat, open tube diffusion procedure was performed. However, not all the diffused surfaces were free of pitting. Even with the intermediate  $\text{SiO}_2$  film, As loss was still causing surface disruption.

For those samples with relatively intact surfaces, metal contact structures were made for tests for  $R_c$ . The fabrication procedure is one known as photoresist lift off. A layer of photoresist is applied to the surface of the diffused GaAs wafer and exposed through the contact structure mask. When developed, the photoresist layer has holes in it where MS contacts to the surface are desired. Contact metal, in this case Au, is evaporated over the entire surface. The wafer is then soaked in acetone which dissolves the photoresist and lifts off the unwanted Au.

In order to give a contact pad with much lower sheet resistance than the underlying substrate, a relatively thick layer of Au is needed. This thick layer causes some partial coverage of the edges of the holes in the photoresist layer during evaporation, and so during the acetone soak the gold is not fully lifted off. However, a light brushing with an artist's brush easily removes the unwanted Au and leaves the adhering Au contacts on the surface.

The tests for  $R_c$  on the contacts made to the intact surfaced diffused samples from the second trial diffusion resulted in unexpected high values for  $R_c$  on the order of 10 s of ohms. Also the I-V curves of the two end contacts, with the diffused layer in between acting as a resistor, displayed on a curve tracer did not yield a straight line but instead curves similar to back to back diodes.

A lapping and staining was performed on these wafers using a  $2^\circ$  lapping angle with the following stains:

1. 2 ml  $\text{HNO}_3$   
18 ml  $\text{H}_2\text{O}$   
1 sixpenny Fe nail [27]
2. 20g  $\text{CuSO}_4 \cdot 5\text{H}_2\text{O}$   
1 ml HF  
100 ml  $\text{H}_2\text{O}$  [27, 28]

but no junction was delineated.

At this point it appeared that there were problems with the n-type diffused layer. Therefore, a different contact structure shown in Figure 8 was fabricated on the GaAs surface using Al as the contact metal. This structure was actually intended for making C-V tests on the Schottky barriers. However, when tunneling occurs, capacitance data cannot be taken due to the presence of the tunneling current and so capacitance tests were not performed. Figure 9 shows the I-V curves of the resistance between contacts A and B and A and C taken on the curve tracer.



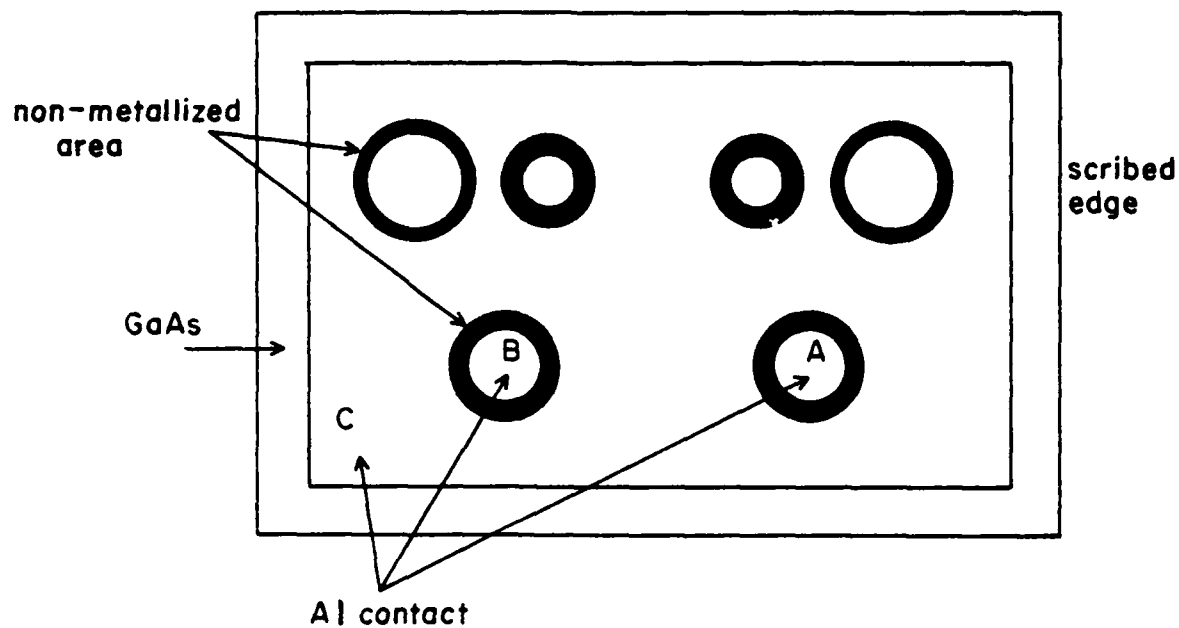


Figure 8. Contact structure used to test for an n-type layer.

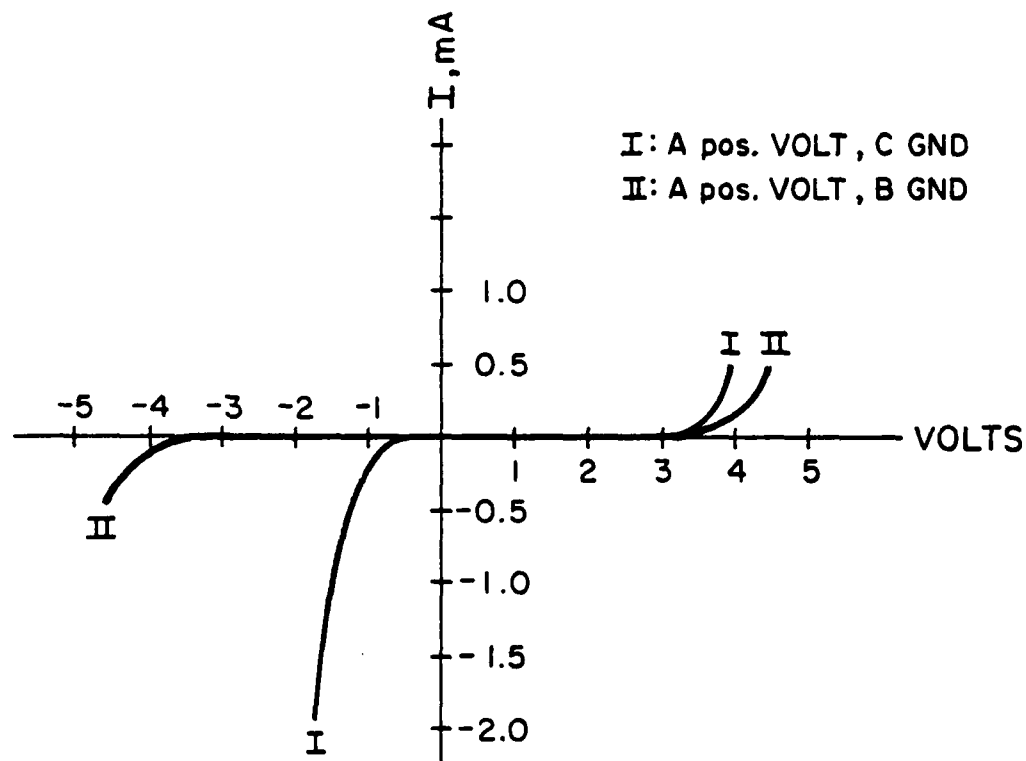


Figure 9. Current-voltage characteristics of the Al contacts A, B, and C on Figure 8.

The curves clearly represent the I-V response of the contacts acting like two back-to-back diodes. The knee represents the reverse bias breakdown region because of the large voltages seen at the point where I starts to increase. In quadrant I of the figure, the curves are essentially the same, giving the reverse I-V response of the same contact in both cases, namely contact A, with contact A at a positive voltage. In quadrant III, case II shows the reverse response for contact B, with B at a positive voltage, and case I for contact C with C positive. Contacts A and B are the same size and should give similar reverse responses. However, the areas of contacts A and C are different. Current, which is proportional to contact area, the reverse leakage of C is much larger than that of B.

The important point is that the curves show reverse bias characteristics for the metal contact when that contact is at a positive voltage. For a MS contact to show a reverse bias characteristic when the metal is positive, it means that the semiconductor must be p-type. In other words, no n-type surface layer exists in the semiconductor.

It was finally decided that the intermediate layer of  $\text{SiO}_2$ , put on to keep the surface intact, was also acting as a barrier to the diffusion of Sn into the surface. Therefore, this intermediate layer must not be used if maximum surface concentration of Sn is to be realized. However, removal of this layer causes increased surface pitting, due to As loss, if the same open boat-open tube diffusion method is used. Therefore, a new diffusion method had to be developed.

Other researchers, when diffusing GaAs wafers, have used either loosely closed quartz boxes [29] or totally closed ampoules [30], instead of the open boat, in a similar open tube furnace. Inside these closed containers, either elemental As or some other source of As is inserted along with the GaAs wafers to be diffused. During the diffusion As escapes from both the wafers and the extra source. Due to the closed nature of the container, an overpressure of As is built up which tends to restrict further loss of As from the wafer surface and reduce the pitting.

Therefore an attempt was made to apply this idea and a semi-closed container (SCC) was built for use in diffusing Sn into the GaAs wafers. Figure 10 shows the container, made from a quartz inner-outer joint with the ends closed down. For the diffusion, the GaAs wafers are covered with the Sn dopant film only and placed in one end of the SCC. The intermediate  $\text{SiO}_2$  layer is not used. This allows the maximum Sn surface concentration to be realized. Pieces of As are placed in the opposite end of the SCC. The same open tube furnace is used. An open boat is used to hold the SCC to allow for easy insertion and removal. Preliminary tests have yielded wafers with intact surfaces (some slight pitting is still seen but should present no problems) and n-type diffused layers of adequate depth.

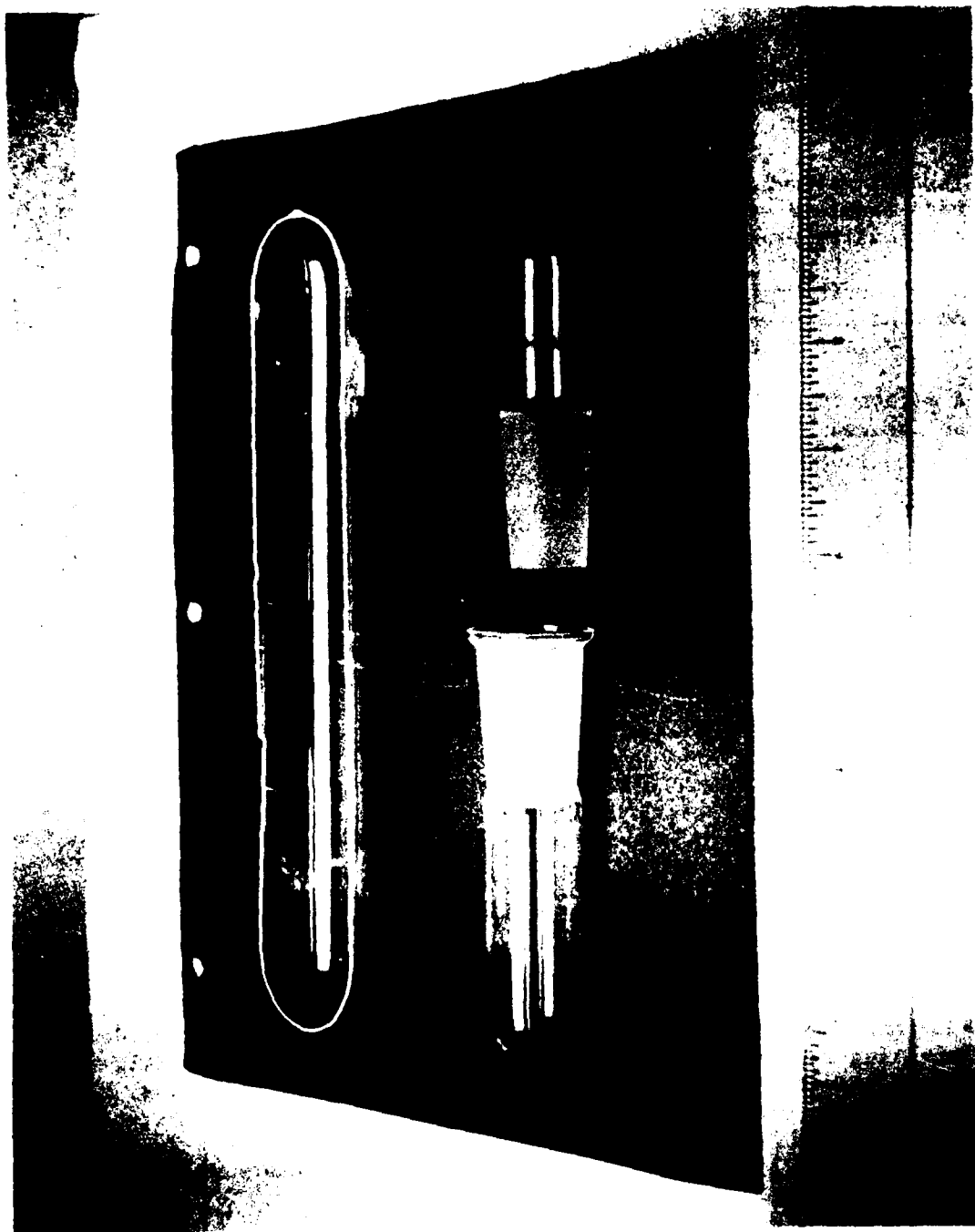


Figure 10. Photograph of the semi-closed chamber used for the diffusion.

#### 4. Summary of first year work and second year plans.

As of the end of the first year of this research program, the following has been accomplished:

- a. A method to investigate tunneling in contacts made on n-type GaAs, utilizing diffused n-type regions to allow control of  $C_s$ , has been developed.
- b. Theoretical models describing tunneling contact performance have been examined and modified to allow their use with the particular fabrication process used in this research.
- c. A successful diffusion process for making Sn doped n-type layers on GaAs has been developed and preliminary tests have shown it yields good results.
- d. A method for making evaporated Au contacts whose structures are delineated by a photoresist lift off technique has been developed.

Plans for research during the second year cover the following:

- a. The diffusions will continue using the SCC method developed. Values of  $C_s$  will be changed by varying source dopant film dilution before spin on or by applying various thicknesses of very thin, intermediate  $\text{SiO}_2$  film. This variation will allow an experimental curve of  $R_c$  vs.  $C_s$  to be developed.
- b. Communication with another colleague has resulted in an idea that perhaps in a lower humidity environment the dopant spin on film will form into a denser glass layer and give better protection against As out diffusion. This idea will be tested to see if it might result in being able to use the open boat-open tube diffusion method again.
- c. An Auger analysis system is now available in the Department of Metallurgy on campus and will be utilized to profile the contacts and perhaps yield a measurement of  $C_s$ .
- d. When more fabrication has been done and it is found that reproducible tunneling contacts can be made using this method; contacts will be tested in other aspects such as lowering of  $R_c$  with annealing, noise performance, etc.
- e. Other methods for relating  $C_s$  to measurable parameters such as  $R_c$  and  $x_j$  will be investigated.

## 5. Appendix

This section describes the basis for the computer programs used to calculate the specific contact resistance,  $R_c$ , of the Au-GaAs contacts. The physical constants used in the formulas are:

$$q = \text{electron charge} = 1.60 \times 10^{-19} \text{ coul.}$$

$$k = \text{Boltzmann's constant} = 1.38 \times 10^{-23} \text{ joule/}^\circ\text{K} \\ \text{or } 8.62 \times 10^{-5} \text{ eV/}^\circ\text{K}$$

$$h = \text{Planck's constant} = 6.625 \times 10^{-34} \text{ joule-sec}$$

$$m^* = \text{effective mass of the conduction band electron in GaAs} \\ = 0.068 \times m_o [9]$$

$$\text{when } m_o = \text{rest mass of the electron} \\ = 9.1 \times 10^{-31} \text{ kg}$$

$$\epsilon_s = \text{dielectric constant for GaAs} = 12 \times \epsilon_o [20] \\ = \text{where } \epsilon_o = 8.85 \times 10^{-14} \text{ F/cm}$$

The parameters for the calculation are:

$$\phi_B = \text{Schottky barrier height} \approx 0.7 - 0.9 \text{ eV} [31, 32]$$

$$T = \text{Temperature}$$

$$C_s = \text{Concentration of Sn dopant at the surface} \\ \text{(but used in this program as the concentration} \\ \text{of a uniformly doped n-type layer)}$$

The first step, and the reason why a computer calculation is used, is in the determination of the fermi potential  $\eta_F = E_F - E_c$  for each choice of  $C_s$ . Usually, the fermi potential  $\eta_F$  is calculated using

$$n = N_c \exp \left( \frac{\eta_F}{kT} \right) \quad (1A)$$

where  $N_c$  is the effective density of states in the conduction band and is given by

$$N_c = 2 \left( \frac{2\pi m^* kT}{h^2} \right)^{2/3} \quad (2A)$$

and  $n$  is the number of free electrons in the conduction band. However, equation (1A) was derived using a simplifying assumption that for most cases  $\eta_F < -3kT$ , and if such is the case when equation (1A) is used, the answer will be accurate. The usual assumption in using equation (1A) is that all the donor atoms in the doped sample are ionized, meaning that the number of free electrons  $n$  is equal to the number of donors. In this case

$$n = C_s$$

A calculation of  $N_c$  is made and  $n/N_c$  is used to find  $\eta_F$ . As long as the resulting  $\eta_F < -3KT$ , the answer for  $\eta_F$  is accurate. The case with GaAs is that because of the small electron effective mass,  $m^*$ , the value of  $N_c$  is rather small. At room temperature

$$N_c \approx 4.7 \times 10^{17}/\text{cm}^3$$

For tunneling in contacts to occur, the doping level,  $C_s$ , must be on the order of  $10^{18}/\text{cm}^3$ , and if complete ionization is assumed, a value of  $\eta_F > 0$  results. This means that equation (1A) can't be used and the more exact formulation must be used.

The more exact calculation uses a summation of the ionized donors (and acceptors if of appreciable concentration) and the available states in the conduction band [34]. The number of free electrons resulting from ionized donors,  $N_D^+$ , is calculated from the total donor doping,  $C_s$ , multiplied by the fermi function.

$$N_D^+ = C_s \left[ \frac{1}{1 + 2 \exp \frac{E_F - E_D}{kT}} \right] \quad (3A)$$

where  $E_D$  is the energy level of the donors.

Part of these free electrons would go to ionizing any acceptor atoms present in the semiconductor. Since in an n-type semiconductor any acceptors present are almost completely ionized, the total number of free electrons would become

$$n = N_D^+ - N_A^- \approx N_D^+ - N_A \quad (4A)$$

where  $N_A$  is the acceptor doping concentration.

In most cases,  $N_D^+ \gg N_A$  and so  $n \approx N_D^+$ .

These free electrons go into conduction band states and the number of electrons in the conduction band states is determined by

$$N = 2 \int_{E=E_c}^{E=\infty} D(E) \frac{1}{1 + \exp \left( \frac{E - E_F}{kT} \right)} dE \quad (5A)$$

At this point, an assumption must be made as to  $D(E)$ . The usual approximations are to assume that a single quantum state needs  $(2\pi)^3/V$  volume in momentum space, a parabolic relationship exists between energy and momentum, and the effective mass at the conduction band edge,  $m^*$ , is valid over the range of integration in which the integrand values are important. This leads to an electron density of states in the conduction band

$$2D(E)dE = V \times N_c \times \frac{2}{\sqrt{\pi}} \left( \frac{E-E_c}{kT} \right)^{\frac{1}{2}} d\left( \frac{E}{kT} \right) \quad (6A)$$

where  $V$  = volume of the semiconductor.

Making a substitution of  $\eta = \frac{E-E_c}{kT}$  and  $n_c = \frac{N}{V}$  = concentration of electrons in the conduction band and using equations (6A) and (5A) gives

$$n_c = N_c \frac{2}{\sqrt{\pi}} \int_{\eta=0}^{\eta=\infty} \sqrt{\eta} \left( \frac{1}{1+\exp\left(\eta - \frac{\eta_F}{kT}\right)} \right) d\eta \quad (7A)$$

Determination of the fermi potential requires a solution which is based upon the fact that  $N_D^+ - N_A$  free electron go into  $n_c$  condition band states. Or

$$C_s \left[ \frac{1}{1+2\exp\left(\frac{\eta_F - \eta_D}{kT}\right)} \right] = N_c \frac{2}{\pi} \int_{\eta=0}^{\eta=\infty} \sqrt{\eta} \left[ \frac{1}{1+\exp\left(\eta - \frac{\eta_F}{kT}\right)} \right] d\eta \quad (8A)$$

letting  $E_F - E_c = \eta_F$  = fermi potential

$E_D - E_c = \eta_D$  = donor potential (for Sn in GaAs  $\eta_D = 5.82$  meV [35])

Given values for  $C_s$  and  $T$ , the computer programs find the simultaneous solution for equation (8A) resulting in a value for  $\eta_F$ . The computer program uses a Simpson approximation [33] for the integral with an upper limit of  $\eta = 10$  instead of  $\eta = \infty$ .

Using the obtained value of  $\eta_F$  along with a chosen parameter,  $\phi_B$ , for the Schottky barrier height, and a calculation of  $E_{oo}$  from

$$E_{oo} = \frac{q\hbar}{2} \sqrt{\frac{C_s}{m^* \epsilon_s}} \quad (9A)$$

the Taylor expansion coefficients  $c_1$  and  $f_1$  are determined from

$$c_1 = \frac{1}{2E_{oo}} \ln \left[ \frac{4\phi_B}{\eta_F} \right] \quad (10A)$$

$$f_1 = \frac{1}{4E_{oo}\eta_F} \quad (10A)$$

Using these constants and the chosen value for T the program calculates to see if

$$1 - c_1 kT > kT \sqrt{2f_1} \quad (11A)$$

is satisfied. If so, the conditions are that the conduction mechanism is by field emission (FE) and the value of contact resistance,  $R_c$ , is calculated from

$$R_c = \left[ \frac{A\pi q}{kT \sin(\pi c_1 kT)} \exp\left(\frac{-\phi_B}{E_{oo}}\right) - \frac{Ac_1 q}{(c_1 kT)^2} \exp\left(\frac{-\phi_B}{E_{oo}} - c_1 \eta_F\right) \right]^{-1} \quad (12A)$$

where

$$A = \frac{4\pi m^* q (kT)^2}{h^3}$$

If equation (11A) is not satisfied then the contact is out of the FE and possibly into the thermionic field emission (TFE) regime. If the inequalities

$$kT > \frac{2E_{oo}}{\left(\ln \frac{4\phi_B}{\eta_F}\right)} \quad (13A)$$

and

$$\frac{\cosh^2\left(\frac{E_{oo}}{kT}\right)}{\sinh^3\left(\frac{E_{oo}}{kT}\right)} < \frac{2(\phi_B + \eta_F)}{3E_{oo}} \quad (14A)$$

are satisfied then the conduction is by TFE and

$$R_c = \left[ \frac{kT}{qA} \right] \frac{E_o}{\sqrt{\pi(\phi_B + \eta_F)E_{oo}}} \left[ \cosh \frac{E_{oo}}{kT} \right] \exp\left(\frac{\phi_B + \eta_F}{E_o} - \frac{\eta_F}{kT}\right) \quad (15A)$$

where

$$E_o = E_{oo} \coth\left(\frac{E_{oo}}{kT}\right)$$



When equation (14A) no longer is satisfied, then the thermionic emission (TE) area is entered with

$$R_c = \frac{kT}{qA} \exp \frac{\phi_B}{kT} \quad (16A)$$

and the contact behavior is rectifying.

## SECTION II

### 1. Introduction

In addition to the work being done in relating theoretical tunneling models to contact performance, the effect of different processing procedures in the generation of surface states on N type GaAs and consequently in the contact behavior is being investigated. An In-Au contact on the same N type GaAs has been developed to be used in the evaluation of the contacts under investigation and because it might have interest in itself as a contact for devices. This section of the report describes work performed from July 1, 1979 through August 31, 1979 and October 1, 1979 through November 30, 1979.

### 2. Theoretical Background

When a metal is evaporated onto N type GaAs, a "pinning" of the fermi level deep into the band gap is invariably observed (in low doped GaAs) no matter which metal is used and which its electronegativity is, as it has been explained in Section I. The band structure appears bent near the surface creating a barrier of typically 0.8V and making the contact to behave as a Schottky barrier.

By 1976, it was clear that there were not intrinsic surface states in the band gap for a (110) surface in GaAs and that there was something else that was causing the bending of the band [7]. When a metal is deposited on a cleaved surface of N-type GaAs equation (110) in an oxygen free ultra high vacuum, it is observed that the evaporation of less than one monolayer is enough to produce the barrier. In the case of Au [7] it is found that the pinning is produced for coverings as small as 0.1 monolayer. It is suggested that since the heat of condensation of Au on Au is quite large (89kcal/mol), the heat of condensation of Au on GaAs will be large too and the released energy might be used to break the bond between the Ga and the As and producing a migration of Ga, leaving behind an As rich surface (non stoichiometric). These suggestions can be checked by forming a Schottky barrier in such a way that defects due to a deficit of one of the constituents can be eliminated. Thus Woodall et al. [36] made a Schottky barrier with Ga onto clean n-type GaAs and no "pinning" was observed. The same has been reported by Bachrach [37] for p-type GaAs.

All this suggests that far before that the Au coverage is enough to have bulk Au characteristics the surface states and the bending of the band they produce are there. The study of the Al deposition on N-type (110) GaAs equation (38) shows that the Al, when evaporated, breaks the GaAs bonds at the surface and that a replacement of Ga by Al takes place even at room temperature, causing a migration of Ga. Another interesting effect is that for thicker layers of metal, Ga is found in the surface and bulk of the metal. In many practical cases, the contact is made from chemically etched GaAs and hence it is also important to look at the effect of the oxygen contamination in the contact characteristic. Spicer et al. [39] have studied the effect of oxygen contamination of clean (cleaved) n-type GaAs (110 orientation).

When the surface is exposed to molecular oxygen, it starts being absorbed by the As (it bonds to the dangling bonds of the As at the surface "chemisorption," without breaking the GaAs molecule. Absorptions of the order of 1% produce important changes in the electronic structure of the GaAs surface modifying the strain present at the surface of the "clean" GaAs and creating unwanted states.

A more drastic phenomenon occurs when the surface is exposed to atomic oxygen. In this case, the oxygen can break the GaAs bond and form true oxides with the Ga and As and thus generate a large amount of acceptor states which produce the bending of the bands and the pinning of the fermi level near the center of the Gap. This effect is also observed whenever the GaAs surface is exposed to molecular O<sub>2</sub> but there is an excitation source (an ion gauge, for example).

### 3. Experimental Method

To study some of these problems, work using Al contacts has been initiated. Al has been chosen because of the difference in the work function between this metal and the GaAs (N-type) is about 0.18eV. Since the observed barrier after the evaporation is about 0.8V any effect due to a change in the preparation conditions can be detected. One aspect that is not desirable in Al is that it can substitute the Ga, forming AlAs. This doesn't happen with Au, but since the difference between the work functions of Au and GaAs (N-type) is around 0.8V it is much more difficult to detect if the main effect causing the barrier are the acceptor states at the interface or the difference in the work function.

Si doped GaAs (N-type, impurity concentration:  $7.10^{17} < N < 3.10^{18} \text{ cm}^{-3}$ ) is being used in the experiments. One first evaporation of Al has been made and the expected 0.8V barrier has been found. The effect of the variations in the preparation procedure is going to be studied.

After a regular cleaning on TCE, Acetone, Methanol and 18 Meg DI water, the samples are etched in:

1:1:4 HCl:MF:DI(H<sub>2</sub>O) with 1 drop of H<sub>2</sub>O<sub>2</sub> for each 10 ml of solution for 1 minute

This etching solution has been reported to minimize surface defects (1). In particular we will study the effect of:

- a) Heating the sample in vacuum before making the contact
- b) Heating the sample in forming gas before making the contact (to see if the H<sub>2</sub> is able to draw part of the oxygen from the surface).
- c) Making the contact in a Ga rich surface.

One first run of case (a) was unsuccessful because of processing problems (etching solution), and a new one is on the way. Al etch cannot be used to etch the Al because it etches the GaAs. HCl and HF based solutions are being

tested. In all samples, the following things will be measured:

Specific resistance of the contact

Barrier height (I-V or C-V method)

I-V characteristic

Auger spectroscopy analysis will be made in an attempt to relate the atomic distribution at the metal-semiconductor interface with the measured characteristic

The annealing effect in each case will be studied

In order to make all these measurements, an ohmic contact to the GaAs is necessary. Because of that some work has been done investigating in contacts with a cover either of Al or Au in order to give them mechanical strength. Previous work by Hakki et al.[40] shows that In-Au structures on GaAs form ohmic contacts when alloyed in forming gas. The reported annealing temperature was 450°C but the optimum temperature was different for different sets of contacts. On the other hand, it has been reported that In-Al contacts sintered at 320°C for 90 sec on rough surfaces produce ohmic contacts of about  $0.1 \Omega \text{ cm}^2$ .

All of our experiments have been made on Si doped N-type GaAs with concentration of impurities between  $7 \cdot 10^{17}$  and  $3 \cdot 10^{18} \text{ cm}^{-3}$ . We made a contact by evaporating first 500Å of In and next 1000Å of Al on a chemically etched surface (1:1:4 HCl:HF:H<sub>2</sub>O for every 10 ml). Annealing at 350°C produced an ohmic contact but some alloying took place and the contact appeared as granulated. Next an In-Au structure was made: We first evaporated 500Å of In and 300Å of Au. The contact test pattern was obtained by a photoresist lift off technique. The contact (as processed) produced a Schottky barrier of about 0.8V. Annealing was performed with gradual variations in time and temperature (in forming gas).

Annealing at 200°C for 10 minutes increased the barrier height slightly. Annealing at 350°C for 15 minutes improved the contact but when further annealed at 375°C for 8 minutes the I-V characteristic became a straight line for current densities of  $12 \text{ A/cm}^2$ . The contact was tested by measuring the I-V characteristic between two contacts ( $0.5 \text{ mm}^2$  each) back to back. The specific contact resistances were in the  $10^{-3} \Omega \text{ cm}^2$  range. Some difficulties were experienced in making good resistance measurements at this point because the gold layer was thin and its own sheet resistance was not negligible.

New evaporations with thicker layer of Au are in progress so that more accurate resistance measurements can be made. The effect of the annealing at higher temperature will also be studied. The auger spectroscopy analysis will be used to study the metal-semiconductor interface at each annealing stage in an attempt to understand this kind of contact.

### SECTION III

#### Optical Measurements

The use of picosecond spectroscopy has proved itself as a valuable tool for analyzing characteristic diffusion length and lifetimes in semiconducting materials. As a result, a picosecond spectroscopy laboratory is being developed in the physics department to probe these properties in the GaAs contact regions. When the contract for this work was eventually approved in April, the spectrometer was immediately ordered. As time progressed, the laboratory was redesigned and facilitated with appropriate electrical and water requirements. However, the July delivery date was extended and as of October 1, 1979, the spectrometer was "due to arrive within the month."

The spectrometer and major support components consists of the following items:

##### Spectra Physics

|           |                           |
|-----------|---------------------------|
| Model 171 | Argon Ion Laser           |
| Model 342 | Acousto-optic mode locker |
| Model 375 | Dye laser                 |
| Model 341 | Synchronous Pump Assembly |
| Model 345 | Cavity Dumper             |

##### NCR

|             |                |
|-------------|----------------|
| Model R8488 | Research table |
|-------------|----------------|

##### Tektronix

|            |                          |
|------------|--------------------------|
| Model 7904 | Sampling Oscilloscope    |
| Model 7A19 | Amplifier Plug in        |
| Model 7S11 | Vertical Sampling Head   |
| Model 7T11 | Horizontal Sampling Head |
| Model S6   | Picosecond Plug in       |

In addition a variety of mirrors, lenses, holders detectors and miscellaneous electronic support equipment has been purchased.

With the arrival of the spectrometer and the completion of the installation and training program, it is anticipated that data will be obtained within six months.

# REFERENCES

1. Anderson, W.T., et.al., IEEE J. Solid State Circ., SC-13, No. 4 (1978) pp. 430-435.
2. Barnes, P.A. and Cho, A.Y., Appl. Phys. Lett., 33, No. 7 (1978) pp. 651-653.
3. DiLorenzo, J.I., Niehaus, W.C., and Cho, A.Y., J. Appl. Phys., 50, No. 2 (1979) pp. 951-954.
4. Inada, T. and Kato, S.J., J. Appl. Phys., 50, No. 6 (1979) pp. 4466-4468.
5. Mozzi, R.L., Fabian, W., and Piekarski, F.J., Appl. Phys. Lett., 35, No. 4 (1979) pp. 337-339.
6. Tsang, W.T., Appl. Phys. Lett., 33, No. 12 (1978) pp. 1022-1025.
7. Lindau, I., et. al., J. Vac. Sci. Technol., 15, No. 4 (1978) pp. 1332-1339.
8. Amith, A. and Mark, P., J. Vac. Sci. Technol., 15, No. 4 (1978) pp. 1344-1352.
9. Sze, S.M., Physics of Semiconductor Devices, Wiley Interscience, New York (1969).
10. Padovani, F.A. and Stratton, R., Solid State Elec., 9 (1966) pp. 695-707.
11. Padovani, F.A., "The Voltage-Current Characteristics of Metal-Semiconductor Contacts," in Semiconductors and Semimetals, Editors: Willardson, R.K. and Beer, A.C., Vol. 7, Part A, Academic Press, New York (1971) pp. 75-146.
12. Price, P. and Radcliffe, J., IBM J. Res. Develop., 3 (1959) p. 364.
13. Harrison, W.A., Phys. Rev., 123 (1961) p. 85.
14. Stratton, R., Lewicki, G., and Mead, C.A., J. Phys. Chem. Solids, 27 (1966) p. 1599.
15. Yu, A.Y.C., Solid State Elec., 13 (1970) pp. 239-247.
16. Cromwell, C.R. and Rideout, V.L., Solid State Elec., 12 (1969) pp. 89-105.
17. Cox, R.H. and Strack, H., Solid State Elec., 10 (1967) pp. 1213-1218.
18. Berger, H.H., J. Electrochem. Soc., 119, No. 4 (1972) pp. 507-514.
19. Hower, P.L., et. al., "The GaAs Field-Effect Transistor," in Semiconductors and Semimetals, Editors: Willardson, R.K. and Beer, A.C., Vol. 7, Part A, Academic Press, New York (1971) pp. 147-200.

20. Grove, A.S., Physics and Technology of Semiconductor Devices, John Wiley and Sons, New York (1967).
21. Kendall, D.L., "Diffusion," in Semiconductors and Semimetals, Editors: Willardson, R.K. and Beer, A.C., Vol. 4, Academic Press New York (1968) pp. 163-259.
22. Irvin, J.C., Bell Sys. Tech. J., 41 (1962) p. 387.
23. Baliga, B.J., Solid State Elec., 20 (1977) pp. 321-322.
24. van der Pauw, L.J., Philips Res. Rept., 13 (1958) pp. 1-9.
25. Purohit, R.K., Phys. Stat. Sol., 24 (1967) p. K57.
26. Sze, S.M. and Irvin, J.C., Solid State Elec., 11 (1968) pp. 599-602.
27. Runyan, W.R., Semiconductor Measurements and Instrumentation, McGraw Hill, New York (1975).
28. Turner, D.R., J. Electrochem. Soc., 106 (1959) pp. 701-705.
29. Gibbon, C.G. and Ketchow, D.R., J. Electrochem. Soc., 118, No. 6 (1971) pp. 975-979.
30. Baliga, B.J. and Ghandi, S.K., J. Electrochem. Soc., 126, No. 1 (1979) pp. 135-138.
31. Pruniaux, B.R., J. Appl. Phys., 42, No. 9 (1971) pp. 3575-3577.
32. Guha, S., Arora, B.M., and Salvi, V.P., Solid State Elec., 20 (1977) pp. 431-432.
33. Squire, W., Integration for Engineers and Scientists, American Elsevier Pub. Co., New York (1970).
34. Spenke, E., Electronic Semiconductors, McGraw Hill, New York (1958).
35. Fetterman, H.R., Appl. Phys. Lett., 21, No. 9 (1972) pp. 434-436.
36. Woodall, J.M., J. Vac. Sci. Technol., 15 (1978) p. 1436.
37. Bachrach, R.Z., J. Vac. Sci. Technol., 15 (1978) p. 1340.
38. Skeath, P., et al., J. Elec. Spect. and Related Phenomena, 17 (1979) p. 259.
39. Spicer, W.E., et al., J. Vac. Sci. Technol., 14 (1977) p. 4.
40. Hakki, B.W., et al., IEEE. Trans. Elec. Dev., ED-13, No. 1, (1966).